

# Axions in Particle Physics and Cosmology

*A Thesis Submitted*

In Partial Fulfillment of the Requirements

For the Degree of

**MASTER OF SCIENCE**

*Submitted By*

**ASHMITA PANDA**



*Under the Guidance of*

**Prof. Amol Dighe**

Department of Theoretical Physics

Tata Institute of Fundamental Research (TIFR), Mumbai

**Dr. Najmul Haque**

Reader-F

School of Physical Sciences

National Institute of Science, Education and Research (NISER), Bhubaneswar

*to the*

**School of Physical Sciences**

**National Institute of Science Education and Research**

Bhubaneswar

19th June, 2023

# **Declaration**

I hereby declare that I am the sole author of this thesis in partial fulfillment of the requirements for an Integrated Masters' degree from National Institute of Science Education and Research (NISER). I authorize NISER to lend this thesis to other institutions or individuals for the purpose of scholarly research.

Signature of Student

Date :

The thesis work reported in the thesis entitled .....  
was carried out under my supervision in the School of ..... at  
NISER, Bhubaneswar, India.

Signature of the Thesis Supervisor

School :

Date :

# Acknowledgement

I would like to express my deep and sincere gratitude to my supervisors Prof. Amol Dighe and Prof. Najmul Haque. The project would not have been possible without their guidance and support. Their expertise in the field allowed me to delve deeper into the subject matter. I also would like to thank Dibya Sankar Chattopadhyay, a PhD student at TIFR, who was constantly available to clarify my doubts and provide valuable feedback.

I would also like to express my gratitude towards the Tata Institute of Fundamental Research (TIFR) administration for allowing me to reside on campus for my project.

Lastly, I would also like to thank my family and my friends at NISER, who constantly stayed by my side and supported me during my difficult days. I will always be grateful to them.

Ashmita Panda  
5th Year Integrated M.Sc.  
School of Physical Sciences  
NISER, Bhubaneswar

# Abstract

Axions are hypothetical elementary particles postulated in 1977 by Roberto Peccei and Helen Quinn as a possible solution to the Strong CP problem, i.e., the problem of non-violation of CP in Quantum Chromodynamics. Since being proposed by Peccei and Quinn, axion has gone on to become a viable candidate of dark matter and dark energy in our Universe due to its non-relativistic nature and extremely weak coupling to Standard Model particles. Thus, there are several experiments which aim to detect axions from various astrophysical sources like stars, globular clusters, supernovae and so on. In this report, I have mainly focussed on the theory of axions and the process of obtaining constraints on interaction strength of axions with Standard Model particles. I have first summarized the Strong CP Problem and the possible solutions to it in the form of axion models. I have then talked about axion as dark matter candidates and the production of axions in the Early Universe. I have then gone over the details of axion-electron and axion-photon interactions. Following that, I have focussed on the formation of axions in the early Universe by the Freeze-in mechanism and obtained their yield by solving the Boltzmann equation. Considering the axions to be dark matter, I have then summarised the process of obtaining constraints on axions using existing constraints on dark matter. To conclude, we obtain constraints on axion interactions with photons and electrons three to four orders of magnitude stronger than the previously existing constraints.

# List of Figures

3.1	Axion-Electron Scattering . . . . .	16
3.2	Axion-Photon Scattering via Triangle Diagram . . . . .	19
3.3	Axion-Photon Scattering via Triangle Diagram . . . . .	20
4.1	Galaxy Rotation Curves . . . . .	25
4.2	Bullet Cluster showing the aftermath of collision of two galaxies . . . . .	26
5.1	Equilibrium distribution ( $Y_{eq}$ ) of Dark Matter obtained from plotting (5.32) . .	35
5.2	Solution for dark matter yield, normalised to equilibrium yield, for $m_\psi = 100\text{GeV}$ by the freeze-out mechanism for different values of scattering cross section. The equilibrium yield plot is also shown for comparison. . . . .	36
5.3	Solution for yield for dark matter of $m_\psi = 100\text{GeV}$ by the freeze-in mechanism for different values of scattering. . . . .	37
5.4	Contours of constant effective dark matter fraction for photophilic and photophobic axions for reheat temperature of $T_{RH} = 5\text{MeV}$ . . . . .	39
6.1	Constraints on Photophilic axion's mass and coupling for irreducible case of $T_{RH} = 5\text{MeV}$ . Plot taken from Langhoff et al . . . . .	43
6.2	Constraints on Photophobic axion's mass and coupling for irreducible case of $T_{RH} = 5\text{MeV}$ . Plot taken from Langhoff et al . . . . .	44

# Contents

	ii
Acknowledgement	ii
Abstract	iii
	Page
<b>1 Introduction</b>	<b>1</b>
<b>2 Axions and the Strong CP Problem</b>	<b>5</b>
2.1 The Strong CP Problem . . . . .	5
2.2 Axions as the Solution to Strong CP Problem . . . . .	8
2.2.1 Peccei-Quinn-Weinberg-Wilczek (PQWW) Axions . . . . .	9
2.2.2 “Invisible” Axion Models . . . . .	10
2.3 Axion Parameters . . . . .	12
2.3.1 Axion Mass . . . . .	12
2.3.2 Axion coupling to photons . . . . .	12
<b>3 Interaction of Axion-like particles</b>	<b>14</b>
3.1 Scattering Cross Section and Decay Rates . . . . .	14
3.2 Decays of Axion-Like-Particles (ALPs) to Electrons . . . . .	15
3.2.1 ALP Electron Interaction . . . . .	15
3.2.2 Decay of ALPs to electron-positron pair . . . . .	18
3.3 Decays of Axion-Like Particles to Photons . . . . .	18
3.3.1 ALP-Photon Interaction . . . . .	18
3.3.2 Decay of ALPs to photons . . . . .	22
<b>4 Axions as Dark Matter</b>	<b>24</b>
4.1 Dark Matter in Cosmology . . . . .	24

4.1.1	Galaxy Rotation Curve . . . . .	24
4.1.2	Bullet Cluster . . . . .	25
4.2	Axion as Dark Matter . . . . .	26
4.2.1	Properties of Axions as Dark Matter . . . . .	26
4.2.2	Axion Production in Cosmology . . . . .	26
4.2.3	Misalignment Mechanism . . . . .	27
<b>5</b>	<b>Dark Matter Cosmology</b>	<b>30</b>
5.1	Boltzmann Equation . . . . .	30
5.2	Freeze-Out and Freeze-in of Dark Matter . . . . .	33
5.2.1	Freeze-Out Scenario . . . . .	35
5.2.2	Freeze-In Scenario . . . . .	37
5.3	Axion Production in the Early Universe . . . . .	38
5.3.1	Solving the Boltzmann equation with relevant scattering processes . . . . .	38
<b>6</b>	<b>Constraints on Axion-Like Particles</b>	<b>41</b>
6.1	The Irreducible Axion Background . . . . .	41
6.2	Constraints from Axion Decays . . . . .	42
<b>7</b>	<b>Conclusion</b>	<b>45</b>

# Chapter 1

## Introduction

Axions are hypothetical pseudo-scalar particles which are theorized to solve the Strong CP problem of the theory of Quantum Chromodynamics. Strong CP is a problem of conservation or non-violation of CP symmetry in strong interactions even though the theory allows for CP violation. There are several possible models for axions and axion-like particles. One class of such models is broadly known as the “invisible-axion models”. The invisible-axion models serve as a solution to the Strong CP problem while also acting as very good dark-matter candidates. Thus it makes the search for axions and axion-like particles, which can act as dark matter particles but don’t necessarily solve the Strong CP problem, an important and exciting problem.

In this thesis, I wish to discuss axions as possible dark matter candidates with emphasis on scattering of axions with photons and electrons, production of axions as dark matter in the Universe by freeze-out and freeze-in mechanism, and constraints obtained on axion couplings by such studies.

I start with a discussion on the Strong CP problem, which is a problem of the theory of Strong interactions. The problem arises due to  $U(1)_A$  symmetry associated with the QCD Lagrangian[1] :

$$\mathcal{L} = -\frac{1}{4}G_a^{\mu\nu}G_{a\mu\nu} + \bar{\psi}_i(i\gamma^\mu(D_\mu)_{ij} - m\delta_{ij})\psi_j. \quad (1.1)$$

The Lagrangian at the classical level has a  $U(1)_A$  symmetry, but the chiral current associated with the symmetry  $j^{\mu 5}$ [2] has a non-zero divergence which cannot be dealt away with like a total derivative term.

$$\partial_\mu j_5^\mu = \frac{1}{32\pi^2}G_a^{\mu\nu}\tilde{G}_{a\mu\nu}. \quad (1.2)$$

This term shows that the  $U(1)_A$  symmetry is not a true symmetry of the system and an extra term needs to be added to the Lagrangian to make it invariant under  $U(1)_A$  transformation :

$$L_\theta = \frac{\theta}{32\pi^2}G_a^{\mu\nu}\tilde{G}_{a\mu\nu}. \quad (1.3)$$

---

The added term  $G\tilde{G}$  is even under charge conjugation but odd under parity transformation. Thus, it is a CP violating term. This term in turn induces an electric dipole moment in the neutron of the order  $d_n \sim \frac{e\theta m_q}{m_n^2}$  [1]. But experimentally, no such dipole moment is observed and the upper limit on  $\theta$  is  $10^{-9}$ . Thus, effectively there is no CP violation observed. This is known as the Strong CP Problem.

Axions were first postulated by Peccei and Quinn[3] to provide viable solutions to the Strong CP problem. They introduced a new global  $U(1)$  symmetry , now known as the  $U(1)_{PQ}$  symmetry to the QCD Lagrangian. The addition of this symmetry promotes  $\theta$  from a static parameter to a dynamical field which preserves CP. This is known as the axion field. The axion then would be the Nambu-Goldstone boson of the broken  $U(1)_{PQ}$  symmetry [3].

There could be various models of QCD axions. The original model was developed by Peccei and Quinn in which they considered the symmetry breaking scale of the  $U(1)_{PQ}$  symmetry to be the scale of electroweak symmetry breaking ( $v_F \approx 250\text{GeV}$ ). To realise the solution, they added another Higgs field to the QCD Lagrangian, making a total of two Higgs fields. This model is also known as the Peccei-Quinn-Weinberg-Wilczek (PQWW) axion [4, 5]. This axion has mass of the order 100keV, but has been ruled out [6] by beam-dump experiments [7] and recent collider experiments too [8].

There also exists another class of axion models, known as the “invisible” axion models, which can be good dark matter candidates along with solving the Strong CP problem. In these models the PQ-symmetry is decoupled from the electroweak scale and gets broken at significantly higher temperatures. This causes the axion to have considerably small mass and coupling. There are two primary models for the “invisible” axion : the Kim-Shifman-Vainshtein-Zakharov (KSVZ) model [9, 10] and the Dine-Fischler-Srednicki-Zhitnitsky (DFSZ) model [11, 12], which I will discuss in this report.

Now as the “invisible” axions like the KSVZ axions are effectively collisionless, they rarely take part in any long-range standard model interaction. Gravitational force is the only significant long-range force. If non-relativistic populations of such axions remain in the Universe, then they can act as extremely good dark matter candidates. Now, if Peccei-Quinn symmetry breaks before inflation, then cold axions may be produced in the early Universe by the realignment of the vacuum by a process known as the misalignment mechanism. These axions have non-relativistic populations and are viable dark matter candidates.

I will also discuss the possibility of axions being produced in the plasma of the Sun by virtue of its interaction to photons. It takes place by a process, known as the Primakoff process [13], in which the photons in the stellar plasma can convert to axions in the presence of electric fields. The transition rate of a photon of energy  $E$  or frequency  $\omega$  into an axion of same

---

energy in the stellar plasma is given as [14]

$$\Gamma_{\gamma \rightarrow a} = \frac{g_{a\gamma}^2 T k_S^2}{32\pi} \left[ \left( 1 + \frac{k_S^2}{\omega^2} \right) \ln \left( 1 + \frac{4\omega^2}{k_S^2} \right) - 1 \right]. \quad (1.4)$$

The flux of such axions produced in the Sun arriving at the Earth can then be obtained. Since most of the energy of the Sun is carried away by photons, the axion luminosity of the Sun cannot exceed the axion luminosity of the Sun. This allows us to place an upper limit of  $g_{\gamma a} \leq 2.4 \times \text{GeV}^{-1}$  on the axion-photon coupling.

Also, axion fluxes on Earth can possibly be detected on Earth by instruments known as Helioscopes which use the Primakoff process to convert axions into high-energy photon beams in the presence of an external magnetic field. One such experiment is known as the CAST (CERN Axion Solar Telescope) experiment which puts constraints on axion-photon coupling as  $g_{a\gamma} < 8.8 \times 10^{-11} \text{GeV}^{-1}$  for a mass limit of  $m_a \leq 0.02 \text{eV}$  [15].

In this report, I will also put emphasis on the scattering of axions with photons and electrons, production of axions as dark matter in the Universe by freeze-out and freeze-in mechanism, and constraints obtained on axion couplings by such studies as reported by Langhoff et al in their recent paper “The Irreducible Axion Background”[16]. The paper strives to put constraints on the couplings of axion-like particles to photons and electrons in two major steps. It first takes into consideration axions produced by the freeze-in mechanism, assuming axions to be a part of dark matter and then it calculates on axion interaction coefficients using the existing constraints on dark matter decays to photons. It allows them to put constraints three to four orders of magnitude stronger than the existing ones for axions in the mass range of 100eV-100MeV.

The paper uses several concepts related to particle physics and cosmology in order to build its arguments. The first major concept is of the theory of axions and the possibility of them being dark matter candidates. The next major concept is of the freeze-in relic density of axions. Freeze-in is a mechanism of forming dark matter in the early Universe in which the density of dark matter particles is almost zero in the beginning, and it never comes into thermal equilibrium with the background. It is the scenario opposite to the Freeze-out mechanism in which dark matter particles in thermal equilibrium with the background decouple from it due to expansion of the Universe. To obtain these relics, one needs to solve the Boltzmann equation which in turn requires one to know the scattering cross section of the particle of interest with other background particles. So, to obtain the freeze-in relic of axions, we need to know the scattering cross-sections of axions with photons and electrons. The paper places its constraints using the decay rates of axions and comparing to the decay rates of dark matter. Thus, along with scattering cross-sections, we also need to know the decay rates of the axions.

In this thesis, I calculate the scattering amplitude and decay rates of  $a \rightarrow ee$  and  $a \rightarrow \gamma\gamma$  decay processes. I also focus on the formation of particles in the early Universe by Freeze-Out

---

and Freeze-In mechanism. I start by discussing the general Boltzmann equation which I then attempt to solve to obtain yields for dark matter particles in general for each case. I then specialise my calculations for axions as dark matter produced by the freeze-in mechanism and try to understand its yield.

In the final chapter, I bring all the above ingredients together to formalise the arguments in the paper[16]. I have also added some chapters as appendices to aid some derivations and concepts.

# Chapter 2

## Axions and the Strong CP Problem

In this chapter, I will summarize the Strong CP problem, the Peccei-Quinn solution and some other viable axion models which have been developed since.

### 2.1 The Strong CP Problem

The Strong CP problem is a problem of the theory of strong interactions. To understand the same, we can start by first writing the QCD Lagrangian,

$$\mathcal{L} = -\frac{1}{4}G_a^{\mu\nu}G_{a\mu\nu} + \bar{\psi}_i(i\gamma^\mu(D_\mu)_{ij} - m\delta_{ij})\psi_j. \quad (2.1)$$

Here,  $\psi_i$  represents the quark field,  $\gamma^\mu$  are the Dirac matrices,  $D_\mu$  is the gauge covariant derivative,  $m$  is the mass matrix for the three quarks and  $G_a^{\mu\nu}$  is the gluon field strength tensor. The indices  $i$  and  $j$  run from 1 to 3 for the three quarks. The index  $a$  runs from 1 to 8 as the  $SU(3)$  gauge group has 8 generators. The gluon field strength tensor is given as :

$$G_{a\mu\nu} = \partial_\mu A_{a\nu} - \partial_\nu A_{a\mu} + g f_{abc} A_{b\mu} A_{c\nu}. \quad (2.2)$$

where,  $A_{a\mu}$  are the gluon fields  $f_{abc}$  are the structure constants of the  $SU(3)$  gauge group.

We ignore the mass of the three light quarks. The QCD Lagrangian has a global  $U(3)_V \times U(3)_A$  symmetry. This is known as the chiral symmetry. It means that in the Lagrangian, in the absence of the mass term, we can make the following replacements :

$$\psi \rightarrow U\psi, \quad \bar{\psi} \rightarrow \bar{\psi}V^\dagger, \quad (2.3)$$

where  $U$  and  $V$  are  $U(3)$  matrices, and leave the Lagrangian invariant.

The current associated with the  $U(1)_A$  symmetry is given as :

$$j_5^\mu = \bar{\psi}\gamma^\mu\gamma^5\psi. \quad (2.4)$$

The derivative of the current (2.4) can be written as [1] :

$$\partial_\mu j_5^\mu = \frac{1}{32\pi^2} G_a^{\mu\nu} \tilde{G}_{a\mu\nu}. \quad (2.5)$$

We see that there exists a non-vanishing anomalous term in the current. Thus, in the limit of massless quarks, even though we supposedly have a  $U(1)_A$  symmetry in the QCD Lagrangian, the anomaly causes us to have a non-zero divergence for the current  $j_5^\mu$ .

More precisely, we can state that the QCD Lagrangian has the global symmetry  $SU(3)_L \times SU(3)_R \times U(1)_V \times U(1)_A$ . The symmetry is spontaneously broken by some order parameter  $\langle \psi_i \bar{\psi}_j \rangle \neq 0$ .  $SU(3)_L \times SU(3)_R$  gets broken down to its diagonal  $SU(3)_D$  and the  $U(1)_A$  symmetry also gets broken [17]. The unbroken symmetry of the system then becomes  $SU(3)_D \times U(1)_V$ . As the  $SU(3)$  group has 8 generators and  $U(1)$  has 1, we expect to observe 9 Goldstone bosons for the 9 broken symmetries. But experimentally, we observe  $\pi^\pm, \pi^0, K^\pm, K^0, \bar{K}^0, \eta$ . The ninth boson is associated with an anomaly.

Explicitly calculating the  $G\tilde{G}$  term in (2.5), we observe that it can be written as a total derivative of some  $K^\mu$  [1], i.e.,

$$G_a^{\mu\nu} \tilde{G}_{a\mu\nu} = \partial_\mu K^\mu, \quad (2.6)$$

where,

$$K^\mu = \epsilon^{\mu\alpha\beta\gamma} A_{a\alpha} \left[ G_{a\beta\gamma} - \frac{g}{3} f_{abc} A_{b\beta} A_{c\gamma} \right]. \quad (2.7)$$

At first glance we might conclude that we can simply redefine the current  $j_5^\mu \rightarrow j_5^\mu - K^\mu$  and obtain  $U(1)_A$  as a symmetry of the Lagrangian as  $\int d^4x G_a^{\mu\nu} \tilde{G}_{a\mu\nu}$  looks like a surface integral which goes to zero at spatial infinity for the boundary condition  $A_a^\mu = 0$ . But, the correct boundary condition to use is that  $A_a^\mu$  should be a pure gauge field at spatial infinity. Thus we should either have  $A_a^\mu = 0$  at spatial infinity, or some gauge transformation of the same. Now as the term  $K^\mu$  has explicit dependence on  $A_a^\mu$  and is not gauge invariant, we cannot set the term  $\int d^4x G_a^{\mu\nu} \tilde{G}_{a\mu\nu}$  to zero. So,  $U(1)_A$  is not a true symmetry of the Lagrangian.

Thus, as a consequence, we need to add an extra term to the QCD Lagrangian, given by :

$$L_\theta = \frac{\theta}{32\pi^2} g_S^2 G_a^{\mu\nu} \tilde{G}_{a\mu\nu}, \quad (2.8)$$

where  $g_S^2$  is a coupling strength associated with the term. The added term  $G\tilde{G}$  is even under charge conjugation but odd under parity transformation. Thus, it is a CP violating term.

The Lagrangian of the system now looks like :

$$\mathcal{L} = -\frac{1}{4} G_{\mu\nu}^a G_a^{\mu\nu} + \bar{\psi}_i \left[ i\gamma^\mu (D_\mu)_{ij} - m\delta_{ij} \right] \psi_j + \frac{\theta}{32\pi^2} g_S^2 G_b^{\mu\nu} \tilde{G}_{b\mu\nu}. \quad (2.9)$$

Considering a two-quark model, we can perform a chiral transformation as :

$$u \rightarrow \exp(i\alpha\gamma_5/2)u \quad , \quad d \rightarrow \exp(i\alpha\gamma_5/2)d. \quad (2.10)$$

Under this chiral transformation, the Lagrangian transforms as :

$$\mathcal{L} \rightarrow \mathcal{L} + \alpha \frac{g_S^2}{32\pi^2} G_b^{\mu\nu} \tilde{G}_{b\mu\nu}. \quad (2.11)$$

So, this is not a true symmetry of the system. But now, due to the  $\mathcal{L}_\theta$  part of the Lagrangian, we can cancel this extra part out by the transforming  $\theta \rightarrow \theta - \alpha$ . The anomalous chiral symmetry of the problem is given as [18]:

$$u \rightarrow \exp(i\alpha\gamma_5/2)u \quad ; \quad d \rightarrow \exp(i\alpha\gamma_5/2)d \quad ; \quad \theta \rightarrow \theta - \alpha. \quad (2.12)$$

As a result of this chiral symmetry, there arises a change in the value of the  $\theta$ . If we consider weak interactions in the system, we need to recall that the quark masses are represented by a complex matrix, i.e.,  $m \equiv (M_{ij})$ . So, the mass part of the Lagrangian can be written as [1] :

$$\mathcal{L}_{mass} = \bar{\psi}_{iR} M_{ij} \psi_{jL} + h.c. \quad (2.13)$$

The important point to note is that the Lagrangian in the current form is not written in the physical basis. To obtain the mass eigenstates of the system we need to diagonalize the mass matrix. In the process of implementing this transformation, the  $\theta$  term changes by  $\arg \det M$  [1], i.e.,

$$\bar{\theta} = \theta + \arg \det M. \quad (2.14)$$

$\bar{\theta}$  is the actual physical parameter that we measure in experiments and it can take any value between  $0 \leq \bar{\theta} \leq 2\pi$ . Then why is the value of  $\bar{\theta}$  so close to zero, forms the statement of the Strong CP Problem.

This term in turn induces an electric dipole moment in the neutron of the order [1] :

$$d_n \sim \frac{e\bar{\theta}m_q}{m_n^2}, \quad (2.15)$$

where,  $m_q$  is the mass of the quark and  $m_n$  is the mass of the neutron. Experimentally, we know the upper bound on  $d_n$  is as follows [1] :

$$|d_n| < 3 \times 10^{-26} e \text{ cm}. \quad (2.16)$$

This then implies an upper limit on  $\bar{\theta}$ , given as :

$$\bar{\theta} \lesssim 10^{-9}. \quad (2.17)$$

There is no apparent reason why the  $\bar{\theta}$  value should be so small. It is a case of extreme fine-tuning and this, in essence, is what we call as the Strong CP problem.

We can have a solution to the Strong CP problem by introducing a new field, the axion field, in the QCD Lagrangian which would dynamically cancel out value of  $\bar{\theta}$  to give a net zero value for the neutron electric dipole moment.

## 2.2 Axions as the Solution to Strong CP Problem

The most widely accepted solution to the Strong CP problem was put forward by Roberto Peccei and Helen Quinn. They introduced a new global  $U(1)$  symmetry, now known as the  $U(1)_{PQ}$  symmetry to the QCD Lagrangian. The addition of this symmetry promotes  $\theta$  from a static parameter to a dynamical field which preserves CP. This is known as the axion field. The axion then would be the Nambu-Goldstone boson of the broken  $U(1)_{PQ}$  symmetry [3].

Under a  $U(1)_{PQ}$  symmetry, the axion field transforms as :

$$a(x) \longrightarrow a(x) + \alpha f_a , \quad (2.18)$$

where,  $f_a$  is an order parameter associated with the breaking of the  $U(1)_{PQ}$  symmetry.

We can write the total Lagrangian including the axion field as [1] :

$$\mathcal{L}_{\text{total}} = \mathcal{L}_{SM} + \theta \frac{g_S^2}{32\pi^2} G_b^{\mu\nu} \tilde{G}_{b\mu\nu} - \frac{1}{2} (\partial_\mu a) (\partial^\mu a) + \xi \frac{a}{f_a} \frac{g_S^2}{32\pi^2} G_b^{\mu\nu} \tilde{G}_{b\mu\nu} + \mathcal{L}_{int} . \quad (2.19)$$

The fourth term in the Lagrangian above involving the  $a/f_a$  factor is the  $U(1)_{PQ}$  symmetry breaking term that leads to the chiral anomaly.  $\mathcal{L}_{int}$  denotes the Lagrangian terms which encapsulate the axion interactions. It will depend on the model chosen.

The last term in 2.19 ensures that the divergence of the  $U(1)_{PQ}$  current takes the form as [1] :

$$\partial_\mu J_{PQ}^\mu = \xi \frac{g_S^2}{32\pi^2} G_b^{\mu\nu} \tilde{G}_{b\mu\nu} . \quad (2.20)$$

The Strong CP problem can be solved dynamically if the axion field has an effective potential such that its minimum occurs at :

$$\langle a \rangle = -\frac{f_a}{\xi} \theta \quad (2.21)$$

Thus, at the minima, the  $\theta$  gets cancelled, providing a dynamical solution to the problem.

In principle,  $\langle a \rangle$  is allowed to take any value in the range  $0 \leq \xi \frac{\langle a \rangle}{f_a} \leq 2\pi$ . The chiral anomaly of QCD generates an effective potential which can be approximated to be periodic in the vacuum angle [1], i.e.,

$$V_{eff} \sim \cos \left[ \bar{\theta} + \xi \frac{\langle a \rangle}{f_a} \right] . \quad (2.22)$$

We can have different axion models based on the form of the effective potential, which in turn would model the axion interactions and the symmetry breaking scale of  $U(1)_{PQ}$ .

### 2.2.1 Peccei-Quinn-Weinberg-Wilczek (PQWW) Axions

This is the original model for axions developed by Peccei-Quinn in their efforts to solve the Strong CP problem. In this model, the  $U(1)_{PQ}$  symmetry breaks down at the scale of electroweak symmetry breaking, i.e.,  $f_a \approx v_F$ , with  $v_F \approx 250\text{GeV}$ .

To realise the Peccei-Quinn solution, an extra Higgs field is added to the QCD Lagrangian, making a total of two Higgs field in the model. We make an assumption that two Higgs fields independently absorb the chiral transformations of the up- and down-quark [4, 5].

Let  $\Phi_u$  be the Higgs field coupling to up-quarks with interaction strength  $f_{ij}^u$  and  $\Phi_d$  be the Higgs field coupling to down-quarks with interaction strength  $f_{ij}^d$ . Here we ignore the couplings to leptons just for simplicity.

We can now write the Yukawa couplings of the Higgs fields and quarks as [4, 5, 1, 18] :

$$\mathcal{L}_{\text{Yukawa}} = f_{ij}^u \bar{q}_{Li} \Phi_u u_{Rj} + f_{ij}^d \bar{q}_{Li} \Phi_d d_{Rj} + h.c. . \quad (2.23)$$

The potential of the Higgs field was chosen by Peccei-Quinn to be [3, 18]:

$$V(\Phi_u, \Phi_d) = -\mu_u^2 \Phi_u^\dagger \Phi_u - \mu_d^2 \Phi_d^\dagger \Phi_d + \sum_{i,j} a_{ij} \Phi_i^\dagger \Phi_i \Phi_j^\dagger \Phi_j + \sum_{i,j} b_{ij} \Phi_i^\dagger \Phi_j \Phi_j^\dagger \Phi_i . \quad (2.24)$$

Here,  $(a_{ij})$ ,  $(b_{ij})$  are real symmetric matrices, and the summation is performed over the Higgs fields of two types.

Let the vacuum expectation value of  $\Phi_u$  and  $\Phi_d$  be given as :

$$\langle \Phi_u^0 \rangle = \frac{v_u}{\sqrt{2}} \quad ; \quad \langle \Phi_d^0 \rangle = \frac{v_d}{\sqrt{2}} . \quad (2.25)$$

Here  $v_u$  and  $v_d$  represent the values at which the Higgs field potentials achieve minima.

From equation (2.23) and (2.24), we can conclude that the full Lagrangian of the system has global  $U(1)_{PQ}$  symmetry.

$$a \longrightarrow a + \alpha v_F , \quad (2.26)$$

$$u_{Rj} \longrightarrow e^{-i\alpha x} u_{Rj} , \quad (2.27)$$

$$d_{Rj} \longrightarrow e^{-i\alpha/x} d_{Rj} , \quad (2.28)$$

$$\Phi_u \longrightarrow e^{i\alpha} \Phi_u , \quad (2.29)$$

$$\Phi_d \longrightarrow e^{i\alpha} \Phi_d , \quad (2.30)$$

where,

$$v_F = \sqrt{v_u^2 + v_d^2} ; \quad x = \frac{v_d}{v_u}. \quad (2.31)$$

The axion field is orthogonal to the longitudinal component of the Z-boson, and it shows up as the common phase field in  $\Phi_u$  and  $\Phi_d$  [1] :

$$\Phi_u = \frac{v_u}{\sqrt{2}} e^{ixa/v_F} ; \quad \Phi_d = \frac{v_d}{\sqrt{2}} e^{ia/xv_F}. \quad (2.32)$$

The PQWW axion would have mass in the order of a 100keV and  $f_a \sim 250\text{GeV}$  such that coupling would be large enough to be detected by experiments. But the model has been ruled out [6] by beam-dump experiments [7] and recent collider experiments too [8].

### 2.2.2 “Invisible” Axion Models

These class of models are called “invisible” axion models as they have extremely weak couplings, i.e.,  $f_a \gg v_F$ . The PQ-symmetry is decoupled from the electroweak scale, unlike the PQWW axion and gets broken spontaneously at a significantly higher temperature. This causes the axion to have considerably decreased mass and coupling. There are two primary modes for the “invisible” axion : the Kim-Shifman-Vainshtein-Zakharov (KSVZ) model [9, 10] and the Dine-Fischler-Srednicki-Zhitnitsky (DFSZ) model [11, 12].

#### Kim-Shifman-Vainshtein-Zakharov (KSVZ) Axion

In the KSVZ axion model [9, 10], no additional Higgs field is added to the Lagrangian, only the standard model Higgs field exists as usual. Instead, a complex scalar field  $\Phi$  with no weak interactions along with a massless fermion field  $\Psi$  is introduced in the Lagrangian. This field  $\Psi$  is an exotic field which is not a part of the Standard Model. The interaction term is written as [19]

$$\mathcal{L}_{KSVZ} = \partial_\mu \Phi^\dagger \partial^\mu \Phi + \left( \frac{i}{2} \bar{\Psi} \partial_\mu \gamma^\mu \Psi + h.c. \right) - h (\bar{\Psi}_L \Phi \Psi_R + h.c.) - V(|\Phi|). \quad (2.33)$$

The potential is chosen to be a “Mexican hat” potential, given as

$$V(|\Phi|) = \frac{\lambda}{4} \left( |\Phi|^2 - \frac{f_{PQ}^2}{2} \right)^2, \quad (2.34)$$

where,  $f_{PQ}$  is the energy scale of the symmetry breaking. The potential has an absolute minima at :

$$|\Phi|_{\min} = \frac{f_{PQ}}{\sqrt{2}}. \quad (2.35)$$

The Lagrangian (2.33) of the system is invariant under the chiral transformation given as :

$$\Phi \longrightarrow e^{i\alpha} \Phi ; \quad \Psi_L \longrightarrow e^{i\alpha/2} \Psi_L ; \quad \Psi_R \longrightarrow e^{-i\alpha/2} \Psi_R. \quad (2.36)$$

The ground state of  $\Phi$  is characterised by this non-vanishing  $|\Phi|$  value given in (2.35) :

$$\langle \Phi \rangle = \frac{f_{PQ}}{\sqrt{2}} e^{i\eta}, \quad (2.37)$$

where  $\eta$  is some arbitrary phase value. The ground state is not invariant under the chiral transformations given in (2.22). We can write it in the form

$$\Phi = \frac{f_{PQ}}{\sqrt{2}} e^{ia/f_{PQ}}. \quad (2.38)$$

The axion field shows up as the phase of the scalar field  $\Phi$ . So, in the ground state, the Lagrangian can be written as [19]

$$\mathcal{L}_{KSVZ} = \partial_\mu \Phi^\dagger \partial^\mu \Phi + \left( \frac{i}{2} \bar{\Psi} \partial_\mu \gamma^\mu \Psi + h.c. \right) - m \bar{\Psi} e^{i\gamma_5 a/f_{PQ}} \Psi, \quad (2.39)$$

such that  $m \equiv h \frac{f_{PQ}}{\sqrt{2}}$ .

So, we see that by construction, the axion field does not interact with standard model particles like quarks or leptons at the tree level. The only interactions it has are with  $\Psi$  which can be taken as some exotic quark. The only explicit standard model coupling it has is via  $a G_b^{\mu\nu} \tilde{G}_{b\mu\nu}$  term in the QCD Lagrangian. It can have interactions with photons but via loop diagrams. The axion can have loop level interactions with standard model quarks via the gluon coupling.

### Dine-Fischler-Srednicki-Zhitnitsky (DFSZ) Axions

In the DFSZ axion model [11, 12], we have two Higgs fields, like the PQWW model. But additionally it also has an electroweak scalar field like the KSVZ model. In this model, there exists tree level couplings of axions to fermions of the standard model. The Lagrangian for the same can be written by a manner similar to done previously for KSVZ and PQWW axions, which has been done in the papers by Michael Dine et al[11] and Zhitnitsky[12].

All these models solve the Strong CP problem, as they ensure that potential of the field gets minimised at  $a/f_a = 0 \bmod 2\pi$  values [6].

## 2.3 Axion Parameters

### 2.3.1 Axion Mass

The mass of the axion can be obtained from its mixing with neutral pion  $\pi^0$ . It can be expressed as [19] :

$$m_a = \frac{f_\pi m_\pi}{f_a} \left( \frac{z}{(1+z+w)(1+z)} \right)^{1/2} = 0.60 \text{eV} \times \frac{10^7 \text{GeV}}{f_a}, \quad (2.40)$$

where,

$$\begin{aligned} f_\pi &\approx 93 \text{MeV} \rightarrow \text{decay constant of pion,} \\ m_\pi &= 135 \text{MeV} \rightarrow \text{mass of pion,} \\ z &= \frac{m_u}{m_d} = 0.58 \pm 0.042 \rightarrow \text{mass ratio of up and down quark,} \\ w &= \frac{m_u}{m_s} = 0.0290 \pm 0.0043 \rightarrow \text{mass ratio of up and strange quark.} \end{aligned}$$

The mass of the axion,  $m_a$  is a model independent quantity as it only depends on ratio of quark masses which is independent of the axion model used. Also, as the  $aG_b^{\mu\nu}\tilde{G}_{b\mu\nu}$  interaction always exists, axions always interact with gluons, and thus to neutral pions via loop diagrams, if required. So, axions always mix with neutral pions and acquire mass via that interaction (like for KSVZ axions). This coupling is independent of the model of the axion [19].

### 2.3.2 Axion coupling to photons

The axion couples to photons via the interaction Lagrangian given as [19] :

$$\mathcal{L}_{int} = -\frac{1}{4}g_{a\gamma}F_{\mu\nu}\tilde{F}_{\mu\nu}a = g_{a\gamma}\mathbf{E}\cdot\mathbf{B}a, \quad (2.41)$$

where  $F$  is the electromagnetic field strength tensor and  $\tilde{F}$  is the dual of the same.

The axion-photon coupling strength is model dependent, and is given as [19] :

$$g_{a\gamma} = -\frac{\alpha}{2\pi f_a} \frac{3}{4} \xi = \frac{m_a/\text{eV}}{0.69 \times 10^{10} \text{GeV}} \xi, \quad (2.42)$$

where,

$$\xi = \frac{4}{3} \left( \frac{E}{N} - \frac{2}{3} \frac{4+z+w}{1+z+w} \right) = \frac{4}{3} \left( \frac{E}{N} - 1.92 \pm 0.08 \right). \quad (2.43)$$

Here  $E$  represents the electromagnetic anomaly and  $N$  represents the color anomaly of the axial current associated with the axion field.

For the DFSZ model, the axion couples to quarks and leptons, thus  $E/N = 8/3$ . For the

KSVZ model, the axion does not couple to leptons, so we have  $E/N = 0$ . We can have other values of  $E/N$  too depending on the model used.

**Conclusion :** Strong CP is a problem of non-violation of the CP parity in strong interactions. In this chapter, we saw how the problem can be solved dynamically by assuming the  $\theta$  parameter to be field instead of a fixed quantity. There can be different models which solve this axion field, out of which the “invisible” axion models remain the most viable. These models could also make axions viable candidates for dark matter due to their weak interactions with other standard model particles.

# Chapter 3

## Interaction of Axion-like particles

In this chapter, we look into the interaction of axions to photons and electrons. These interactions are important for us as they give us a picture of how axions may have formed in the early Universe and how can they decay to observable Standard Model particles.

So, to understand these interactions, I will discuss decay rates, scattering cross-sections, scattering amplitudes and attempt to calculate the decay rates of axions to photons and electrons. Studying the decay rates of axion-like particles allows us to estimate the flux of Standard Model particles like photons and electrons, produced in the process. We can then attempt to design experiments to look for these byproducts of ALP decays as an indirect method of detecting axionic dark matter.

### 3.1 Scattering Cross Section and Decay Rates

In this section I will talk about the general prescription for calculating scattering cross sections and decay rates.

The decay rate for a particle is the probability per unit time that the particle will decay or disintegrate. The scattering cross section is a measure of the probability that a certain process will occur when incident radiation or particles fall on localized particles. For example, the probability of two protons colliding when two proton beams are accelerated towards each other.

To calculate both these quantities, we need to know the amplitude  $\mathcal{M}$  for the process and the phase space available in the process. The amplitude gives us the probability of the transition happening.

Say we have a decay event happening like  $1 \rightarrow 2 + 3 + 4 + \dots$ . Then the decay rate is given

as :

$$\Gamma = \frac{s}{2m_1} \int (2\pi)^4 \delta^4(p_1 - p_2 - p_3 - p_4 - \dots) |\mathcal{M}|^2 \prod_{j=2}^n \Theta(p_j^0) (2\pi) \delta(p_j^2 - m_j^2) \frac{d^4 p_j}{(2\pi)^4}. \quad (3.1)$$

Here,  $s$  is the symmetry factor to account for over counting,  $|\mathcal{M}|$  is the scattering amplitude and  $\Theta$  is a Heaviside step function. The delta function ensures that the overall momentum is conserved in the event while the Heaviside step function ensures that the energy remains positive. The second delta function  $\delta(p_j^2 - m_j^2)$  ensures that the products formed are on-shell particles.

We can now attempt to simplify the expression. Using the expression

$$\delta(x^2 - a^2) = \frac{1}{2a} [\delta(x - a) + \delta(x + a)]. \quad (3.2)$$

This allows us to remove the Heaviside step function as follows :

$$\Theta(p^0) \delta(p^2 - m^2) = \Theta(p_j^0) \delta(p_0^2 - \vec{p}^2 - m^2) = \frac{1}{2\sqrt{\vec{p}^2 + m^2}} \delta(p_0 - \sqrt{\vec{p}^2 + m^2}). \quad (3.3)$$

Now, if we integrate over  $dp_j^0$ , the delta function would kill the integral and we will be left with an expression for decay rate as :

$$\Gamma = \frac{s}{2m_1} \prod_{j=2}^n \int \frac{d^3 \vec{p}_j}{(2\pi)^3} (2\pi)^4 \frac{\delta^4(p_1 - p_2 - \dots - p_n)}{2\sqrt{\vec{p}^2 + m^2}} |\mathcal{M}|^2. \quad (3.4)$$

Similarly, the scattering cross section can be written as :

$$\sigma = \frac{s}{4\sqrt{(p_1 \cdot p_2)^2 - (m_1 m_2)^2}} \prod_{j=3}^n \frac{d^3 \vec{p}_j}{(2\pi)^3} \frac{(2\pi)^4 \delta^4(p_1 + p_2 - p_3 - p_4 - \dots - p_n)}{2\sqrt{\vec{p}_j^2 + m^2}}. \quad (3.5)$$

## 3.2 Decays of Axion-Like-Particles (ALPs) to Electrons

In this section I will calculate the scattering amplitudes and decay rates of axions decaying to electrons. To characterize the interactions, I will use the Lagrangian given as [16] :

$$\mathcal{L} \supset \frac{1}{2} (\partial_\mu a)^2 - \frac{1}{2} m_a^2 a^2 + \bar{e} (i \not{D} - m_e) e - \frac{1}{4} F_{\mu\nu} F^{\mu\nu} - \frac{1}{4} g_{a\gamma\gamma} a F_{\mu\nu} \tilde{F}^{\mu\nu} + \frac{g_{aee}}{2m_e} (\partial_\mu a) \bar{e} \gamma^\mu \gamma^5 e. \quad (3.6)$$

### 3.2.1 ALP Electron Interaction

The interaction of the axion with the electron is a derivative interaction in the axion[16] :

$$\mathcal{L} \supset \frac{g_{aee}}{2m_e} (\partial_\mu a) \bar{e} \gamma^\mu \gamma^5 e. \quad (3.7)$$

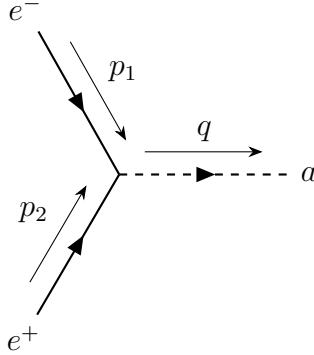


**Fig. 3.1:** Axion-Electron Scattering

Using Feynman rules, I can write  $|\mathcal{M}|$  as :

$$\mathcal{M} = \frac{-ig_{aee}}{2m_e} \bar{v}(p_2)\gamma^\mu\gamma^5 u(p_1).iq_\mu. \quad (3.8)$$

Squaring the above term :

$$|\mathcal{M}|^2 = \frac{g_{aee}^2}{4m_e^2} \left\{ v^\dagger(p_2)\gamma^0\gamma^\mu\gamma^5 u(p_1)q_\mu \right\} \left\{ q_\nu u^\dagger(p_1) (\gamma^5)^\dagger (\gamma^\nu)^\dagger (\gamma_0)^\dagger v(p_2) \right\}.$$

Recalling the properties of the gamma matrices :

$$\{\gamma^\mu, \gamma^\nu\} = 2g^{\mu\nu} \quad ; \quad \{\gamma^5, \gamma^\mu\} = 0, \quad (3.9)$$

we can evaluate the scattering amplitude.

$$\begin{aligned} \implies |\mathcal{M}|^2 &= \frac{g_{aee}^2}{4m_e^2} \left\{ \bar{v}(p_2)\gamma^\mu\gamma^5 u(p_1)q_\mu \right\} (-1) \left\{ q_\nu u^\dagger(p_1) \gamma^5 \gamma^0 \gamma^\nu v(p_2) \right\}, \\ \implies |\mathcal{M}|^2 &= \frac{g_{aee}^2}{4m_e^2} \left\{ \bar{v}p_2\gamma^\mu\gamma^5 u(p_1)q_\mu \right\} \left\{ q_\nu \bar{u}(p_1) \gamma^5 \gamma^\nu v(p_2) \right\}, \end{aligned}$$

Summing over all possible diagrams :

$$\begin{aligned} \implies \sum |\mathcal{M}|^2 &= \frac{g_{aee}^2}{4m_e^2} \sum_{s_2, s_1} \bar{v}^{s_2}(p_2)\gamma^\mu\gamma^5 u^{s_1}(p_1)q_\mu q_\nu \bar{u}^{s_1}(p_1) \gamma^5 \gamma^\mu v^{s_2}(p_2), \\ \implies \sum |\mathcal{M}|^2 &= \frac{g_{aee}^2}{4m_e^2} \text{Tr} \left[ (\not{p}_2 - m_e) \gamma^\mu \gamma^5 q_\mu q_\nu (\not{p}_1 + m_e) \gamma^\nu \gamma^5 \right], \\ \implies \sum |\mathcal{M}|^2 &= \frac{g_{aee}^2}{4m_e^2} \text{Tr} \left[ (\not{p}_2 - m_e) \not{q} \gamma^5 \not{q} (\not{p}_1 + m_e) \gamma^5 \right], \\ \implies \sum |\mathcal{M}|^2 &= \frac{g_{aee}^2}{4m_e^2} \text{Tr} \left\{ (\not{p}_2 - m_e) \not{q} (\gamma^5)^2 (-1) \not{q} (-\not{p}_1 + m_e) \right\}, \\ \implies \sum |\mathcal{M}|^2 &= -\frac{g_{aee}^2}{4m_e^2} \text{Tr} \left[ (\not{p}_2 - m_e) \not{q}^2 (-\not{p}_1 + m_e) \right]. \end{aligned}$$

Using the momentum conservation at the vertex, we have  $p_1 + p_2 = q$ , so we can write

$q_\mu \gamma^\mu = \not{p}_1 + \not{p}_2$  (let  $p_1 \equiv p$ ).

$$\begin{aligned} &\implies \sum |\mathcal{M}|^2 = -\frac{g_{aee}^2}{4m_e^2} \text{Tr} \left[ -\not{p}_2 \not{p}_1 \not{q}^2 + \not{p}_2 \not{q}^2 m_e + m_e \not{q}^2 \not{p}_1 - m_e^2 \not{q}^2 \right], \\ &\implies \sum |\mathcal{M}|^2 = \frac{g_{aee}^2}{4m_e^2} \text{Tr} \left[ \not{p}_2 \not{p}_1 \not{q} \right] + m_e^2 \frac{g_{aee}^2}{4m_e^2} \cdot 4m_a^2, \\ &\implies \sum |\mathcal{M}|^2 = \frac{g_{aee}^2}{4m_e^2} \text{Tr} \left[ \not{p}_1 \not{q}^3 - \not{p}_1 \not{q}^2 \right] + g_{aee}^2 m_a^2, \\ &\implies \sum |\mathcal{M}|^2 = \frac{g_{aee}^2}{4m_e^2} \text{Tr} [\gamma^\mu \gamma^\nu \gamma^\rho \gamma^\sigma p_\mu q_\nu q_\rho q_\sigma] - \frac{g_{aee}^2}{4m_e^2} \text{Tr} [\gamma^\mu \gamma^\nu \gamma^\rho \gamma^\sigma p_\mu p_\nu q_\rho q_\sigma] + g_{aee}^2 m_a^2. \end{aligned}$$

Using the values of traces of gamma matrices[2] :

$$\begin{aligned} &\implies \sum |\mathcal{M}|^2 = -4 \frac{g_{aee}^2}{4m_e^2} (g^{\mu\nu} g^{\rho\sigma} - g^{\mu\rho} g^{\nu\sigma} + g^{\mu\sigma} g^{\nu\rho}) p_\mu p_\nu q_\rho q_\sigma \\ &\quad + 4 \frac{g_{aee}^2}{4m_e^2} (g^{\mu\nu} g^{\rho\sigma} - g^{\mu\rho} g^{\nu\sigma} + g^{\mu\sigma} g^{\nu\rho}) p_\mu q_\nu q_\rho q_\sigma + g_{aee}^2 m_a^2, \\ &\implies \sum |\mathcal{M}|^2 = -4 \frac{g_{aee}^2}{4m_e^2} [(p.p)(q.q) - (p.q)(p.q) + (p.q)(p.q)] \\ &\quad + 4 \frac{g_{aee}^2}{4m_e^2} [(p.q)(q.q) - (p.q)(q.q) + (p.q)(q.q)] + g_{aee}^2 m_a^2 \\ &\implies \sum |\mathcal{M}|^2 = -\frac{g_{aee}^2}{m_e^2} m_e^2 m_a^2 + \frac{g_{aee}^2}{m_e^2} (p.q) m_a^2 + \frac{g_{aee}^2}{m_e^2} m_e^2 m_a^2. \end{aligned}$$

We finally obtain the scattering cross section as :

$$\therefore \sum |\mathcal{M}|^2 = \frac{g_{aee}^2}{m_e^2} (p.q) m_a^2.$$

Now, if we consider an axion decaying to an electron and a positron, and we go to the centre of momentum frame, then  $\vec{q} = 0$  (before decay). Thus, we can write :

$$p.q = p_0 q_0 - |\vec{p}| |\vec{q}| \cos \theta = p_0 q_0.$$

Also in the centre of momentum frame after the collision,  $\vec{p}_1 + \vec{p}_2 = 0$ . Using overall momentum conservation :

$$p_1 + p_2 = q \implies (p_1^0 + p_2^0, \vec{p}_1 + \vec{p}_2) = (q_0, 0) \implies (q_0, \vec{q}) = (2p_0, 0).$$

Thus, we obtain :

$$p.q = p_0 \cdot q_0 = 2p_0^2 = 2m_e^2.$$

So, we obtain the final expression for the scattering amplitude as[16] :

$$\therefore |\mathcal{M}|^2 = 2g_{aee}^2 m_a^2. \quad (3.10)$$

### 3.2.2 Decay of ALPs to electron-positron pair

The decay rate of axion like particles can now be found using the formula (3.4). We will use the symmetry factor as  $s = 1/2$ .

$$\begin{aligned}\Gamma &= \frac{1}{4m_a} \int \frac{d^3 p_1}{(2\pi)^3} \frac{d^3 p_2}{(2\pi)^3} (2\pi)^4 \frac{\delta^4(p_a - p_1 - p_2)}{2\sqrt{\vec{p}_1^2 + m_e^2} 2\sqrt{\vec{p}_2^2 + m_e^2}} |\mathcal{M}|^2, \\ \implies \Gamma &= \frac{2g_{aee}^2 m_a}{4m_a^2} \int \frac{d^3 p_1}{(2\pi)^3} \frac{(2\pi)\delta(p_a^0 - p_1^0 - p_2^0)}{4(\vec{p}^2 + m_e^2)}, \\ \implies \Gamma &= \frac{g_{aee}^2 m_a}{2} \int (4\pi) \vec{p}^2 \frac{d\vec{p}_1}{(2\pi)^3} \frac{(2\pi)\delta(p_a^0 - p_1^0 - p_2^0)}{4(\vec{p}^2 + m_e^2)}.\end{aligned}$$

Performing calculations in the centre of momentum frame of the decaying ALP, we can write  $p_1^0 = p_2^0 = E_1$ ,  $p_a^0 = m_a$ . Now using the relation between  $\vec{p}$  and energy :

$$E_1^2 = \vec{p}_1^2 + m_e^2 \implies E_1 dE_1 = \vec{p}_1 d\vec{p}_1.$$

Replacing  $\vec{p}_1$  with  $E_1$  :

$$\begin{aligned}\implies \Gamma &= \frac{g_{aee}^2 m_a (4\pi)(2\pi)}{2(2\pi)^3} \int \frac{\vec{p}_1 E_1 \delta(m_a - 2E_1)}{4E_1^2} dE_1, \\ \implies \Gamma &= \frac{g_{aee}^2 m_a (4\pi)(2\pi)}{2(2\pi)^3} \int \frac{\sqrt{E_1^2 - m_e^2} \delta(m_a - 2E_1)}{4E_1} dE_1.\end{aligned}$$

Using the delta function to kill the integral :

$$\implies \Gamma = \frac{g_{aee}^2 m_a}{2\pi} \frac{1}{2m_a} \sqrt{\frac{m_a^2}{4} - m_e^2}.$$

So, we finally obtain the decay rate of axion like particles as :

$$\Gamma_{a \rightarrow e^+ e^-} = \frac{g_{aee}^2 m_a}{8\pi} \sqrt{1 - \frac{4m_e^2}{m_a^2}} \Theta(m_a - 2m_e). \quad (3.11)$$

The Heaviside step function ensures  $m_a \geq 2m_e$  and that the process is allowed kinematically.

## 3.3 Decays of Axion-Like Particles to Photons

In this section I will calculate the scattering amplitudes and decay rates of axions decaying to photons.

### 3.3.1 ALP-Photon Interaction

The axion interacts with a photon via electrons through a triangle diagram.

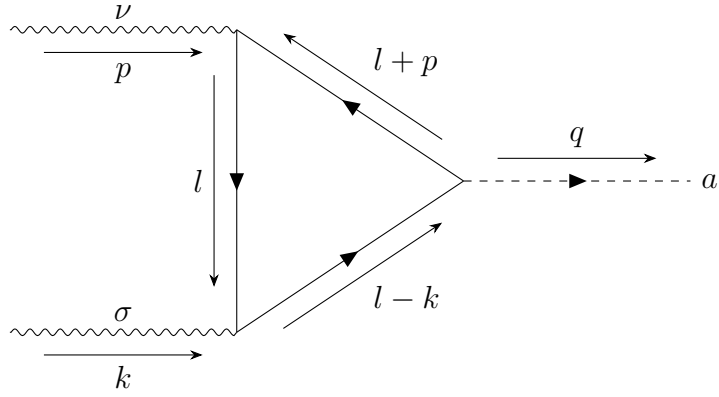


**Fig. 3.2:** Axion-Photon Scattering via Triangle Diagram

Using the Feynman rules, the we can write[2] :

$$\begin{aligned} \mathcal{M} &= (iq_\mu) \cdot \left\{ \frac{(-ig_{aee})}{2m_e} (-ie)^2 \int \frac{d^4 l}{(2\pi)^4} \left[ \gamma^\mu \gamma^5 \cdot \frac{i(l-k)}{(l-k)^2} \gamma^\sigma \frac{i l}{l^2} \gamma^\nu \frac{i(l+p)}{(l+p)^2} \right] \right\}, \\ \implies \mathcal{M} &= (iq_\mu) \cdot \left\{ \frac{(-ig_{aee})}{2m_e} (-ie)^2 \int \frac{d^4 l}{(2\pi)^4} \text{Tr} \left[ \gamma^\mu \gamma^5 \cdot \frac{i(l-k)}{(l-k)^2} \gamma^\sigma \frac{i l}{l^2} \gamma^\nu \frac{i(l+p)}{(l+p)^2} \right] \right\}. \end{aligned}$$

Using momentum conservation at vertex 1 :

$$\begin{aligned} q^\mu + (l^\mu - k^\mu) &= l^\mu + p^\mu \\ \implies q_\mu \gamma^\mu \gamma^5 &= (l_\mu + p_\mu - l_\mu + k_\mu) \gamma^\mu \gamma^5, \\ \therefore q_\mu \gamma^\mu \gamma^5 &= (l_\mu + p_\mu) \gamma^\mu \gamma^5 + \gamma^5 (l_\mu - k_\mu) \gamma^\mu. \end{aligned}$$

Using this in the expression for  $\mathcal{M}$  :

$$\begin{aligned} \mathcal{M} &= i \frac{-ig_{aee}}{2m_e} (-ie)^2 \int \frac{d^4 l}{(2\pi)^4} \left\{ \text{Tr} \left[ (l+p) \gamma^5 \cdot \frac{i(l-k)}{(l-k)^2} \gamma^\sigma \frac{i l}{l^2} \gamma^\nu \frac{i(l+p)}{(l+p)^2} \right] \right. \\ &\quad \left. + \text{Tr} \left[ \gamma^5 (l-k) \frac{i(l-k)}{(l-k)^2} \gamma^\sigma \frac{i l}{l^2} \gamma^\nu \frac{i(l+p)}{(l+p)^2} \right] \right\}. \end{aligned} \quad (3.12)$$

Focussing on the  $(l+p)^2$  terms :

$$(l+p)^2 = \gamma^a \gamma^c l_a l_c + \gamma^a \gamma^d l_a p_d + \gamma^b \gamma^c p_b l_c + \gamma^b \gamma^d p_b p_d.$$

Writing the  $\gamma$  terms as :

$$\gamma^a \gamma^c = \frac{\{\gamma^a, \gamma^c\} + [\gamma^a, \gamma^c]}{2} = \frac{2\eta^{ac} + [\gamma^a, \gamma^c]}{2}. \quad (3.13)$$

Now, the commutator is given as :

$$[\gamma^a, \gamma^c] = \begin{cases} 0 & : a = c \\ 0 & : a = 0, c \neq 0 \text{ or } a \neq 0, c = 0 \\ [\sigma^a, \sigma^c] = 2i\epsilon^{abc}\sigma^b & : a \neq c, a \neq 0, c \neq 0 \end{cases} \quad (3.14)$$

Now,  $\text{Tr}(2i\epsilon^{abc}\sigma^b) = 0$ . Thus, the commutator of  $\gamma$  matrices is traceless. So now, we can use the property of trace to simplify (3.11). In the second term in (3.11), we first push  $\gamma^\sigma$  through  $\gamma^5$  and then use the property of trace. We also replace  $\not{l}$  by  $(\not{l} + \not{k})$  in the first term of (3.11)[2].

$$\therefore \mathcal{M} = \frac{ig_{aee}}{2m_e} e^2 \int \frac{d^4 l}{(2\pi)^4} \text{Tr} \left[ \gamma^5 \frac{\not{l}}{l^2} \gamma^\sigma \frac{(\not{l} + \not{k})}{(l + k)^2} \gamma^\nu - \gamma^5 \frac{\not{l}}{l^2} \gamma^\nu \frac{(\not{l} + \not{k})}{(l + p)^2} \gamma^\sigma \right]. \quad (3.15)$$

This above expression gives in contribution from only one diagram. It is antisymmetric under the exchange of  $(p, \nu)$  and  $(k, \sigma)$ , which implies that the term might add to zero when taking both diagrams into consideration.

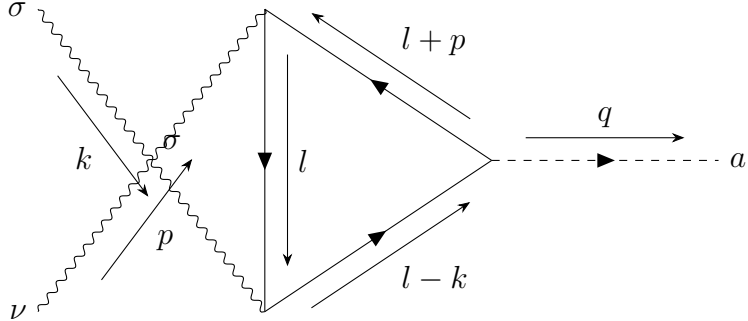


**Fig. 3.3:** Axion-Photon Scattering via Triangle Diagram

But the issue here is that the integral being shifted is divergent. So, the shifting must come with some cost. To calculate that, we start with the definition of  $\gamma^5$  in d-dimensions[2].

$$\gamma^5 = i\gamma^0\gamma^1\gamma^2\gamma^3. \quad (3.16)$$

$\gamma^5$  anticommutes with  $\gamma^\mu$  for  $\mu = 0, 1, 2, 3$  and commutes with  $\gamma^\mu$  for other values of  $\mu$  [2]. Then, we can write the internal line momenta in terms of 4 dimensional component and  $(d - 4)$  dimensional component [2].

$$l = l_\parallel + l_\perp. \quad (3.17)$$

Using this definition, we can rewrite  $q_\mu \gamma^\mu \gamma^5$  as [1]:

$$\therefore q_\mu \gamma^\mu \gamma^5 = (\not{l} + \not{k}) \gamma^5 + \gamma^5 (\not{l} - \not{p}) - 2\gamma^5 l_\perp. \quad (3.18)$$

The third term then gives a non-zero contribution when we evaluate  $\mathcal{M}$  which can be written as [2]:

$$\mathcal{M} = \frac{ie^2 g_{aee}}{2m_e} \int \frac{d^4 l}{(2\pi)^4} \text{Tr} \left[ -2\gamma^5 l_\perp \frac{(l-k)}{(l-k)^2} \gamma^\sigma \frac{l}{l^2} \gamma^\nu \frac{(l+p)}{(l+p)^2} \right]. \quad (3.19)$$

The above integral can be evaluated to obtain the result given as [2] :

$$\therefore \mathcal{M} = \frac{ie^2 g_{aee}}{2m_e} \left( \frac{-i}{2(4\pi)^2} \right) \text{Tr} [2\gamma^5 (-k) \gamma^\sigma p^\nu] = \frac{-ie^2 g_{aee}}{2m_e} \frac{1}{4\pi^2} \epsilon^{\alpha\sigma\beta\nu} k_\alpha p_\beta. \quad (3.20)$$

Squaring the above term gives us the desired scattering amplitude.

$$\begin{aligned} |\mathcal{M}|^2 &= \frac{e^4 g_{aee}^2}{4m_e^2} \frac{1}{16\pi^4} \epsilon^{\alpha\sigma\beta\nu} k_\alpha p_\beta \epsilon_{a\sigma b\nu} k^a k^b, \\ \implies |\mathcal{M}|^2 &= \frac{e^4 g_{aee}^2}{4m_e^2} \frac{1}{16\pi^4} \times 4 \left( \delta_{ab}^{\alpha\beta} k_\alpha p_\beta k^a p^b - \delta_{ba}^{\alpha\beta} k_\alpha p_\beta k^a p^b \right), \\ \implies |\mathcal{M}|^2 &= \frac{e^4 g_{aee}^2}{4m_e^2} \frac{1}{16\pi^4} \times 4 [(k.k)(p.p) - (p.k)^2]. \end{aligned}$$

Using momentum conservation of the overall process ( $p + k = q$ ) :

$$\begin{aligned} \implies |\mathcal{M}|^2 &= \frac{e^4 g_{aee}^2}{4m_e^2} \frac{1}{16\pi^4} \times 4 [(k.k)(p.p) - \{p.(q-p)\}^2], \\ \implies |\mathcal{M}|^2 &= \frac{e^4 g_{aee}^2}{4m_e^2} \frac{1}{16\pi^4} \times 4 [m_\gamma^4 - (p.q - p.p)^2]. \end{aligned}$$

Here  $m_\gamma$  is known as the thermal mass of the photon. It is the mass obtained by the photon when it travels through a background of thermal particles. It is determined to be

$m_\gamma \simeq eT/3 \simeq T/10$  [16]. Now using the calculation similar to the electron case, we can write  $p.q = \frac{q_0^2}{2} = \frac{m_a^2}{2}$ .

$$\begin{aligned} \implies |\mathcal{M}|^2 &= \frac{e^4 g_{aee}^2}{4m_e^2} \frac{1}{16\pi^4} \times 4 \left[ m_\gamma^4 - \left( \frac{m_a^2}{2} - m_\gamma^2 \right)^2 \right], \\ \implies |\mathcal{M}|^2 &= \frac{e^4 g_{aee}^2}{4m_e^2} \frac{1}{16\pi^4} \times 4 \left[ m_\gamma^4 - \left( \frac{m_a^4}{4} + m_\gamma^4 - m_\gamma^2 m_a^2 \right) \right], \\ \implies |\mathcal{M}|^2 &= \frac{e^4 g_{aee}^2}{4m_e^2} \frac{1}{16\pi^4} \times 4 \left[ \frac{-m_a^2}{4} (m_a^2 - 4m_\gamma^2) \right]. \end{aligned}$$

Thus, we can finally write it as [16] :

$$|\mathcal{M}|^2 = -\frac{e^4 g_{aee}^2}{4m_e^2} \frac{1}{16\pi^4} m_a^2 (m_a^2 - 4m_\gamma^2). \quad (3.21)$$

### 3.3.2 Decay of ALPs to photons

The decay rate of axion-like particles to photons can be calculated in the similar way. It is given as[16] :

$$\Gamma = \frac{m_a^3}{64\pi} \left| g_{a\gamma\gamma} - \frac{\alpha g_{aee}}{m_e \pi} (1 - \tau f^2(\tau)) \right|, \quad (3.22)$$

where,

$$\tau = \left( \frac{2m_e}{m_a} \right)^2, \quad (3.23)$$

$$f(\tau) = \begin{cases} \sin^{-1}\left(\frac{1}{\sqrt{\tau}}\right) & : \tau \geq 1 \\ \frac{\pi}{2} + \frac{i}{2} \ln\left(\frac{1 + \sqrt{1 - \tau}}{1 - \sqrt{1 - \tau}}\right) & : \tau < 1 \end{cases} \quad (3.24)$$

We can take two extreme cases, either  $m_a \ll m_e$  or  $m_a \gg m_e$ .

**Case 1 :  $m_a \ll m_e$**  In this case, the axion-like particle cannot decay to electrons. The contribution from electrons comes from a triangle loop diagram which allows axion-like particles to decay to photons.

For  $m_a \ll m_e$  we have  $\tau \gg 1$  which would then imply that  $\tau^{-1/2} \ll 1$ . Now we can expand the inverse sin function as :

$$f(\tau) = \sin^{-1}\left(\frac{1}{\sqrt{\tau}}\right) \simeq \frac{1}{\sqrt{\tau}} + \frac{1}{6} \cdot \left(\frac{1}{\sqrt{\tau}}\right)^3 + \text{higher order terms}. \quad (3.25)$$

Using this expansion and ignoring all higher order terms, we can write :

$$1 - \tau f^2(\tau) = -\frac{1}{3\tau} = -\frac{m_a^2}{12m_e^2}. \quad (3.26)$$

Plugging this in (3.22), we get the decay rate as :

$$\Gamma_{a \rightarrow \gamma\gamma} = \frac{m_a^3}{64\pi} \left[ g_{a\gamma\gamma} + \frac{\alpha g_{aee} m_a^2}{12m_e^3 \pi} \right]. \quad (3.27)$$

**Case 2 :  $m_a \gg m_e$**  : In this case, the axion-like particle can decay to electrons, along with photons.

In this limit as  $\tau \rightarrow 0$ , we have  $1 - \tau f^2(\tau) \simeq 1$ . Thus, we get the decay rate as :

$$\Gamma_{a \rightarrow \gamma\gamma} = \frac{m_a^3}{64\pi} \left[ g_{a\gamma\gamma} - \frac{\alpha g_{aee}}{\pi m_e} \right]^2. \quad (3.28)$$

**Conclusion :** The decay channel of axion-like particles to photons and electrons are relevant as they can form important astrophysical signatures. Also, the scattering amplitudes calculated in this section are used to solve the Boltzmann equation which in turn gives us the yield of axion-like particles in the early Universe.

# Chapter 4

## Axions as Dark Matter

The nature of dark matter is one of the biggest unsolved problems in physics currently. In this chapter, I will review what is dark matter, the observational evidences of dark matter and will try to motivate why axions can be good dark matter candidates via its production mechanism in the early Universe.

### 4.1 Dark Matter in Cosmology

Dark matter is a hypothetical form of matter that is believed to account for 85% of the matter of the Universe. It is known as “dark” matter as it has no interaction with electromagnetic field. The only way it interacts with other matter is via the gravitational field.

We have several observational evidences that motivate and support the existence of this unknown dark matter.

#### 4.1.1 Galaxy Rotation Curve

The advent of radio telescopes made it possible for us to measure the rotational velocity of cylindrically symmetric galaxies, like spiral galaxies. Observations are made using the Doppler shift of 21cm hyperfine line of neutral hydrogen.

Let  $R$  be the radius of the galaxy and  $M$  be the total mass enclosed. Also, let  $r$  be the distance from the centre and  $M(r)$  be the mass enclosed till radius  $r$ . If we assume the galaxy to be a homogenous sphere with density  $\rho$  and radius  $R$ . Thus, we can write the rotational velocity as [20] :

$$v(r) = \sqrt{\frac{4\pi G\rho}{3}}r \quad : \quad r \leq R, \quad (4.1)$$

$$v(r) = \sqrt{\frac{GM}{r}} \quad : \quad r > R. \quad (4.2)$$

So, we expect a linear relationship between  $v$  and  $r$  for inside the galaxy and then  $v$  should fall off as  $r^{-1/2}$ . We expect that most of the matter of the galaxy should be contained in the galactic bulge close to the centre. So, the disk portion of the galaxy should have velocity decreasing with radial distance from the centre.

But experimentally we observe that the galaxy rotation curve flattens out instead of showing a  $r^{-1/2}$  fall.

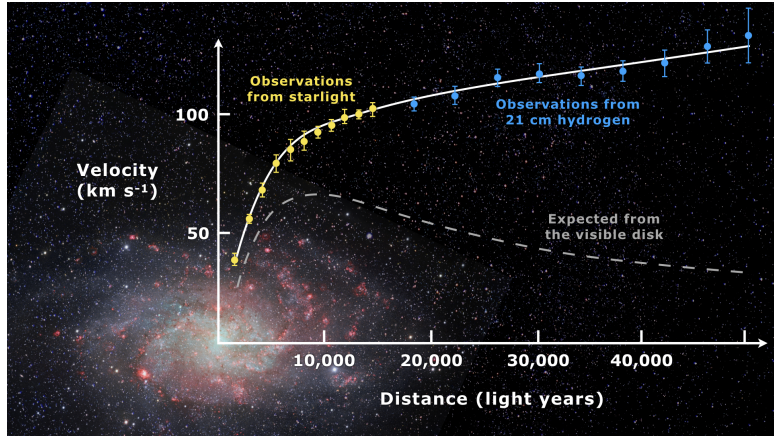


Fig. 4.1: Galaxy Rotation Curves [21]

This rotation curve can be explained by assuming there is a significant amount of matter outside the central bulge of the galaxies that is not luminous. This is what we call as the dark matter.

### 4.1.2 Bullet Cluster

The bullet cluster consists of two cluster of galaxies colliding with each other. It provides us with the best evidence of the existence of dark matter.

Assuming there are three components of each galaxy, the stars, the gas representing the baryonic matter and the hypothetical dark matter, we do observe each component behaving differently during the collision.

Stars are least affected by the collision and mostly pass through each other. They just slow down due to gravitational interaction. Baryonic matter or the gases of the colliding galaxies interact electromagnetically, and they get slowed down much more in comparison to the stars. Gravitational lensing can be used to detect the presence or absence the hypothetical dark matter. Modified Newtonian Dynamics (MOND) theory is an alternative theory to the dark matter hypothesis that attempts to explain the observed galactic curves by proposing modifications to the Newton's law of gravitation. If Modified Newtonian Dynamics (MOND) theories could explain the properties of galaxies, then gravitational lensing should follow the trend of the baryonic matter in the bullet cluster. But we observe that lensing is strongest

near the regions separated after the collision, i.e., closer to the visible mass than the X-ray halo (baryonic matter).

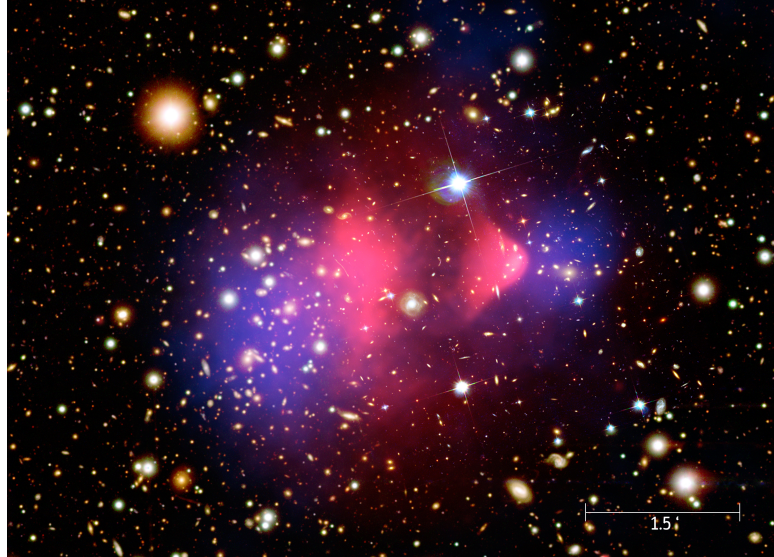


**Fig. 4.2:** Bullet Cluster showing the aftermath of collision of two galaxies [22][23]

Thus, most of the mass of the cluster is localised in two “dark” matter regions away from the gas. Thus, they must have been only weakly interacting via gravity. This further supports the theory of dark matter.

## 4.2 Axion as Dark Matter

### 4.2.1 Properties of Axions as Dark Matter

Cold dark matter has two defining properties which are also satisfied by the axion, i.e.,

- i.) It is possible for a non-relativistic population of axions to be present in our Universe to produce the estimated dark matter density.
- ii.) The “invisible” axions, like the KSVZ axions are effectively collisionless. They rarely take part in any long-range standard model interaction. Gravitational force is the only significant long-range force.

Even though axions are extremely light particles with mass given as (2.40), they can be produced out-of-equilibrium as non-relativistic cold populations.

### 4.2.2 Axion Production in Cosmology

Axion production in the Universe has two important scales associated with it. The first is the temperature  $T_{PQ}$  at which the Peccei-Quinn symmetry breaks. We can have different

mechanisms of axion production depending on whether this  $T_{PQ}$  is greater or less than the reheat temperature of the Universe after inflation. The second scale is the temperature at which the axion acquires a non-zero mass arising due to non-perturbative QCD effects[18].

The Peccei-Quinn symmetry is broken at temperatures less than  $T_{PQ}$ . At early times when the temperature of the Universe is greater than  $T_{PQ}$ , the symmetry remains unbroken and axions are not produced.  $T_{IRh}$  denotes the inflationary reheat temperature of the Universe. We can have two main cases involving  $T_{PQ}$  and  $T_{IRh}$  :

**Case 1.  $T_{PQ} > T_{IRh}$**  : In this case, the Peccei-Quinn symmetry is broken before the Universe could go into the inflationary phase. Thus, the axion field gets homogenized with only a single value over the entire visible Universe [24].

**Case 2.  $T_{PQ} < T_{IRh}$**  : In this case, the Peccei-Quinn symmetry breaking occurs during the inflation of the Universe. The axion field does not get homogenized over space and it exists like a topological defect in space. The topological defects are the configuration of axion fields between two regions with different values of the same[24, 25].

### 4.2.3 Misalignment Mechanism

This is one of the simplest models of axion formation in the Early Universe which says that cold axions can be formed independent of the reheat temperature by realignment of the vacuum. The only condition that it needs to satisfy is that  $T_{PQ} > T_{IRh}$ , i.e., inflation occurs with reheat temperature smaller than  $T_{PQ}$  [24].

For simplicity, let us consider an axion model with an extra complex scalar field  $\phi(x)$ . Writing the “Mexican hat” potential for the said scalar field [18] :

$$V(|\phi|) = \frac{\lambda}{4} (|\phi|^2 - f_a^2)^2 , \quad (4.3)$$

where,  $f_a$  is the axion decay constant. When the temperature of the Universe becomes comparable to  $f_a$ , i.e.,  $T_{\text{Universe}} \sim T_{PQ} \sim f_a$ ,  $\phi$  acquires the vacuum expectation value given as :

$$\langle \phi \rangle = f_a e^{i\theta(x)} . \quad (4.4)$$

Here  $\theta(x)$  is related to the axion field as :

$$a(x) = f_a \theta(x) . \quad (4.5)$$

After the temperature of the universe becomes comparable to the QCD confinement scale, i.e.,  $T_{\text{Universe}} \sim \Lambda_{QCD}$ , the axion obtains a mass due to non-perturbative QCD effects. The dynamics of the axion field can now be estimated by the Klein-Gordon equation in the

Friedmann-Robertson-Walker (FRW) metric. Recalling (2.22), the effective potential can be estimated as [18] :

$$V_{eff}(\theta) \sim m_a(T(t))f_a^2(1 - \cos \theta). \quad (4.6)$$

Here  $m_a(T(t))$  represents the mass of the axion which depends on the temperature which in turn depends on the time.

The equation of motion for the axion in the FRW metric can be written as:

$$\ddot{\theta} + 3H(t)\dot{\theta} + m_a^2(T(t))\sin \theta = 0. \quad (4.7)$$

As the Peccei-Quinn symmetry breaking occurred before inflation, the only mode of the axion we should be concerned about the zero mode, i.e.,  $\theta \approx 0$ . In this limit, we have  $\sin \theta \approx \theta$ . We can re-write the equation of motion (4.7) as :

$$\ddot{\theta} + 3H(t)\dot{\theta} + m_a^2(t)\theta = 0. \quad (4.8)$$

When the Universe cools down to a critical temperature  $T_1$ , we can define a corresponding critical time ( $t_1$ ) as :

$$m_a(T_1(t_1))t_1 = 1. \quad (4.9)$$

It is the time at which the mass of the axion turns on. The dependence of mass on the temperature is given as [24] :

$$m_a(T) \simeq 4 \times 10^{-9} \text{eV} \times \left( \frac{10^{12} \text{GeV}}{f_a} \right) \left( \frac{\text{GeV}}{T} \right)^4. \quad (4.10)$$

The temperature and time can be related using the Hubble rate, and using the definition of critical time (4.9), we can obtain  $t_1$  as [24] :

$$t_1 \simeq 2 \times 10^{-7} \text{sec} \left( \frac{f_a}{10^{12} \text{GeV}} \right). \quad (4.11)$$

This gives us the order of the momentum of the axion field as :

$$p_a(t_1) \sim \frac{1}{t_1} \sim 10^{-9} \text{eV} \quad \text{with } f_a \simeq 10^{12} \text{GeV}. \quad (4.12)$$

So, we can see that the axion population is non-relativistic and it can be a valid dark matter candidate. [18]

The energy density of the scalar field around the minima of the potential is given as [18] :

$$\rho = \frac{f_a^2}{2} \left\{ \dot{\theta}^2 + m_a^2(t)\theta^2 \right\}. \quad (4.13)$$

Then by the Virial theorem, we can write :

$$\langle \dot{\theta}^2 \rangle = m_a^2 \langle \theta^2 \rangle = \frac{\rho}{f_a^2}. \quad (4.14)$$

We can also estimate the density using the scale factor of expansion  $R(t)$  and the fact that the axions are non-relativistic and decoupled from the background metric :

$$\rho \propto \frac{m_a(t)}{R^3(t)}. \quad (4.15)$$

If the axion mass varies adiabatically, the number of axions per comoving volume remains conserved. So, the initial energy density can be written from (4.14) as :

$$\rho_1 = \frac{1}{2} f_a^2 m_a^2(t_1) \theta_1^2, \quad (4.16)$$

where,  $\theta_1$  is the initial angle of the axion field, also known as the “misalignment” angle. Thus, the axion density at present time, labelled by  $\rho_0$  can be estimated using (4.15) :

$$\rho_0 = \rho_1 \frac{m_a(t_0)}{m_a(t_1)} \frac{R^3(t_1)}{R^3(t_0)}. \quad (4.17)$$

Using the expression for  $\rho_1$  from (4.16) in (4.17) along with the definition of critical time in (4.9), we obtain :

$$\rho_0 = \frac{1}{2} f_a^2 \frac{m}{t_1} \left( \frac{R(t_1)}{R(t_0)} \right)^3 \theta_1^2, \quad (4.18)$$

where,  $t_0$  denotes present time. Thus, we can make an estimate for the axion density in the present as a function of the misalignment angle and the axion decay constant  $f_a$ .

**Conclusion :** So, from this chapter, we can conclude that the axion population of the Universe is non-relativistic, and it has a non-zero density of the axion in present time. As viable axion models have very small couplings, the oscillations do not decay away. Thus, axion could be a viable dark matter candidate.

# Chapter 5

## Dark Matter Cosmology

In this chapter, I will discuss the process of dark matter production in the early Universe by the freeze-out and freeze-in mechanism, then the corresponding production of axions by the freeze-in mechanism as discussed in the paper “The Irreducible Axion Background” by Langhoff et al[16].

### 5.1 Boltzmann Equation

Assuming the standard model of cosmology, we can write the expansion rate of the Universe as  $H$ , interaction rate per particle for reactions maintaining thermal equilibrium to be  $\Gamma$  and the scale factor to be  $a$ . Then, the particles decouple from the background when  $\Gamma \leq H$ . The evolution of a particle’s phase space distribution function is controlled by the Boltzmann equation, which can be written as[26] :

$$\hat{L}[f] = \hat{C}[f], \quad (5.1)$$

where,  $\hat{C}$  is the collision operator .  $\hat{L}$  is known as the Liouville operator. In the non-relativistic case it can be written as :

$$\hat{L}_{NR} = \frac{d}{dt} + \frac{d\vec{x}}{dt} \cdot \vec{\nabla}_x + \frac{d\vec{v}}{dt} \cdot \vec{\nabla}_v = \frac{d}{dt} + \vec{\nabla} \cdot \vec{\nabla}_x + \frac{\vec{F}}{m} \cdot \vec{\nabla}_v. \quad (5.2)$$

For the relativistic case, it can be written as :

$$\hat{L}_R = p^\alpha \frac{\partial}{\partial x^\alpha} - \Gamma_{\beta\gamma}^\alpha p^\beta p^\gamma \frac{\partial}{\partial p^\alpha}. \quad (5.3)$$

In the Friedmann-Lemaitre-Robertson-Walker metric, the phase space density is homogenous and isotropic. So, we have the Liouville operator as :

$$\hat{L}[f(E, t)] = E \frac{\partial f}{\partial t} - \frac{\dot{a}}{a} |\vec{p}|^2 \frac{\partial f}{\partial E}, \quad (5.4)$$

where  $f(E, t)$  is the distribution function of the particle  $\psi$  that we are considering. We can write the number density as :

$$n(t) = \frac{g}{(2\pi)^3} \int d^3 p f(E, t). \quad (5.5)$$

Now, using (5.4), we can write Boltzmann equation as :

$$\frac{\partial f}{\partial t} - \frac{\dot{a}}{a} \frac{|\vec{p}|^2}{E} \frac{\partial f}{\partial E} = \frac{\hat{C}[f]}{E}. \quad (5.6)$$

Integrating the Boltzmann equation by parts :

$$\frac{g}{(2\pi)^3} \int d^3 p \frac{\partial f}{\partial t} - \frac{\dot{a}}{a} \frac{g}{(2\pi)^3} \int d^3 p \frac{|p|^2}{E} \frac{\partial f}{\partial E} = \frac{g}{(2\pi)^3} \int d^3 p \frac{\hat{C}[f]}{E}.$$

Using  $|\vec{p}|^2 = 3pE$ , we get the final equation as :

$$\frac{dn}{dt} + 3 \frac{\dot{a}}{a} n = \frac{g}{(2\pi)^3} \int d^3 p \frac{\hat{C}[f]}{E}. \quad (5.7)$$

We can now focus on the collision terms. Say we have a collision of the form :

$$\psi + a + b \longrightarrow i + j + \dots . \quad (5.8)$$

We can then write the RHS of (5.7) as :

$$\begin{aligned} \frac{g}{(2\pi)^3} \int \hat{C}[f] \frac{d^3 p_\psi}{E_\psi} &= - \int d\Pi_\psi d\Pi_a d\Pi_b \dots d\Pi_i d\Pi_j \dots \times (2\pi)^4 \delta^4(p_\psi + p_a + p_b + \dots - p_i - p_j - \dots) \\ &\times [ |\mathcal{M}|_{\psi+a+b \rightarrow i+j+\dots}^2 f_a f_b f_\psi (1 \pm f_i)(1 \pm f_j) \dots \\ &- |\mathcal{M}|_{i+j+\dots \rightarrow \psi+a+b}^2 f_i f_j \dots (1 \pm f_a)(1 \pm f_b)(1 \pm f_\psi) ], \end{aligned} \quad (5.9)$$

where,

$$d\Pi = g \frac{1}{(2\pi)^3} \frac{d^3 p}{2E}. \quad (5.10)$$

To simplify the equation, we will start by assuming T or CP invariance, i.e.,

$$|\mathcal{M}|_{i+j+\dots \rightarrow \psi+a+b}^2 = |\mathcal{M}|_{\psi+a+b \rightarrow i+j+\dots}^2 \equiv |\mathcal{M}|^2. \quad (5.11)$$

We can simplify the equation further by considering Maxwell-Boltzmann distribution for all species instead of separate Fermi-Dirac and Bose-Einstein statistics.

$$1 \pm f \simeq 1 \quad ; \quad f_i(E_i) = \exp \left[ -\frac{(E_i - \mu_i)}{T} \right]. \quad (5.12)$$

Then, the final Boltzmann equation for all species in kinetic equilibrium can be written as :

$$\begin{aligned}\dot{n}_\psi + 3Hn_\psi &= - \int d\Pi_\psi d\Pi_a d\Pi_b \cdots d\Pi_i d\Pi_j \cdots (2\pi)^4 |\mathcal{M}|^2 \\ &\times \delta^4(p_i + p_j + \cdots - p_\psi - p_a - p_b) [f_a f_b f_\psi - f_i f_j \cdots].\end{aligned}\quad (5.13)$$

The term  $3Hn_\psi$  accounts for the dilution due to expansion of the Universe, where  $H$  is the Hubble expansion rate. The right hand side indicates the change in the number of  $\psi$  particles due to interactions. We now wish to consider the evolution of number of particles in a comoving volume. Using entropy density  $s$ , as entropy is conserved per comoving volume, we can define :

$$Y = \frac{n_\psi}{s}. \quad (5.14)$$

Using the fact that entropy is conserved in a comoving volume, we can write :

$$sa^3 = c \implies \frac{n_\psi}{Y} a^3 = c.$$

Taking time derivative :

$$\implies \frac{\dot{n}_\psi}{Y} a^3 - \frac{n_\psi}{Y^2} \dot{Y} a^3 + \frac{n_\psi}{Y} 3a^2 \dot{a} = 0.$$

We finally obtain the equation :

$$\therefore \dot{n}_\psi + 3Hn_\psi = s\dot{Y}. \quad (5.15)$$

Now, as the interaction terms usually depend explicitly on temperature, we can introduce an independent variable :

$$x = \frac{m}{T}. \quad (5.16)$$

During the radiation dominated era, the time and ‘x’ are related as [26]:

$$t = 0.301 g_*^{-\frac{1}{2}} \frac{m_{Pl}}{T^2} = 0.301 g_*^{-\frac{1}{2}} \frac{m_{Pl}}{m^2} x^2, \quad (5.17)$$

where,  $m_{Pl} = 2.176 \times 10^{-8}$  kg is the Planck mass and  $g_*$  is given as :

$$g_* = \sum_{i \in \text{bosons}} g_i \left( \frac{T_i}{T} \right)^4 + \frac{7}{8} \sum_{i \in \text{fermions}} g_i \left( \frac{T_i}{T} \right)^4. \quad (5.18)$$

Converting the time derivative to a derivative of x, we obtain the left hand side of the Boltzmann equation (5.13, 5.15) as :

$$s\dot{Y} = \frac{s}{2x c_1} \frac{dY}{dx} ; \quad c_1 = 0.301 g_*^{-1/2} \frac{m_{Pl}}{m^2}, \quad (5.19)$$

where,  $c_1$  is a constant arising from the relation between  $t$  and  $x$ . The Boltzmann equation

can now then be written as :

$$\frac{dY}{dx} = -\frac{x}{sH(m)} \int \Pi_\psi \Pi_a \Psi_b \cdots d\Pi_i d\Pi_j \cdots (2\pi)^4 |\mathcal{M}|^2 \times \delta^4(p_i + p_j + \cdots - p_\psi - p_a - p_b) [f_a f_b f_\psi - f_i f_j \cdots], \quad (5.20)$$

where,

$$H(m) = \frac{1}{2c_1} = \frac{1}{2 \times 0.301} g_*^{\frac{1}{2}} \frac{m^2}{m_{Pl}} = 1.67 g_*^{\frac{1}{2}} \frac{m^2}{m_{Pl}} ; \quad H(x) = H(m)x^{-2}. \quad (5.21)$$

## 5.2 Freeze-Out and Freeze-in of Dark Matter

If massive particle species remained in thermal equilibrium with the background till present time, their abundance would get exponentially suppressed as the number density can be written as [26] :

$$\frac{n}{s} \sim \left(\frac{m}{T}\right)^{3/2} \exp\left(-\frac{m}{T}\right). \quad (5.22)$$

Thus, their present day abundance would become negligible due to exponential. So, if we want a species to have some significant relic abundance, they need to freeze out or fall out of equilibrium as a temperature when  $m/T$  is not that large.

Let us consider a stable species with lifetime comparable or more than the age of the Universe. We can consider only annihilation and inverse annihilation as the relevant process.  $\psi$  represents the dark matter species and  $X$  represents the Standard Model species, like electrons, photons, neutrinos etc.



For simplification, we assume there is no asymmetry between  $\psi$  and  $\bar{\psi}$ . We also assume that  $X$  and  $\bar{X}$  have thermal distribution with zero chemical potential.

We can now recall the Boltzmann equation (5.20) and write it for our specific case :

$$\frac{dY}{dx} = -\frac{x}{sH(m)} \int \Pi_\psi \Pi_{\bar{\psi}} d\Pi_X d\Pi_{\bar{X}} (2\pi)^4 |\mathcal{M}|^2 \delta^4(p_X + p_{\bar{X}} - p_\psi - p_{\bar{\psi}}) [f_\psi f_{\bar{\psi}} - f_X f_{\bar{X}}]. \quad (5.24)$$

We can now focus on the last term of the above equation (5.24). As  $X, \bar{X}$  are in thermal equilibrium :

$$f_X = \exp(-E_X/T) ; \quad f_{\bar{X}} = \exp(-E_{\bar{X}}/T).$$

From the delta function, we know that :

$$E_X + E_{\bar{X}} = E_\psi + E_{\bar{\psi}}.$$

Thus we finally obtain :

$$f_X f_{\bar{X}} = \exp \left[ -\frac{(E_X + E_{\bar{\psi}})}{T} \right] = \exp \left[ -\frac{(E_\psi + E_{\bar{\psi}})}{T} \right] = f_\psi^{Eq} f_{\bar{\psi}}^{Eq}. \quad (5.25)$$

Using this, and the definition of number density of a particle given as :

$$n = \frac{g}{(2\pi)^3} \int d^3 p f(p). \quad (5.26)$$

We can write the final Boltzmann equation as :

$$\frac{dY}{dx} = -\frac{x \langle \sigma_{\psi\bar{\psi} \rightarrow X\bar{X}} \rangle s}{H(m)} (Y^2 - Y_{Eq}^2), \quad (5.27)$$

where  $\langle \sigma_{\psi\bar{\psi} \rightarrow X\bar{X}} \rangle$  is the scattering cross section given as :

$$\langle \sigma_{\psi\bar{\psi} \rightarrow X\bar{X}} \rangle = \left( n_\psi^{Eq} \right)^{-2} \int \Pi_\psi \Pi_{\bar{\psi}} d\Pi_X d\Pi_{\bar{X}} (2\pi)^4 |\mathcal{M}|^2 \delta^4(p_X + p_{\bar{X}} - p_\psi - p_{\bar{\psi}}) \exp \left[ -\frac{(E_\psi + E_{\bar{\psi}})}{T} \right]. \quad (5.28)$$

For non-relativistic cases ( $x \geq 3$ ), the cross section can have velocity dependence, and consequently temperature dependence as :

$$\langle \sigma v \rangle \propto v^p ; \quad \langle v \rangle \propto T^{1/2} \implies \langle \sigma v \rangle \propto T^{p/2} \equiv T^n.$$

We have s-wave annihilation for  $n=0$  ( $p=0$ ) and p-wave annihilation for  $n=1$  ( $p=2$ ). We can write the cross section as :

$$\langle \sigma v \rangle = \sigma_0 x^{-n}. \quad (5.29)$$

Now entropy depends on temperature as  $s \propto T^3 \implies s \propto x^{-3}$ , the coefficient  $(-x\sigma_0 x^{-n}s)$  in (5.27) has a total  $x^{-n-2}$  dependence. So, we can write the Boltzmann equation as :

$$\frac{dY}{dx} = -\lambda x^{-n-2} (Y^2 - Y_{Eq}^2); \quad \lambda = \sqrt{\frac{8\pi^2}{45} g_*(x) m_{Pl} m_\psi \langle \sigma v \rangle}. \quad (5.30)$$

Plugging in all the values, we can write the final Boltzmann equation for  $n = 0$  as :

$$\frac{dY}{dx} = -\sqrt{\frac{8\pi^2}{45} g_*(x) m_{Pl} m_\psi} \frac{\langle \sigma v \rangle}{x^2} (Y^2 - Y_{Eq}^2), \quad (5.31)$$

where  $m_{Pl}$  is the Planck mass,  $m_\psi$  is the dark matter mass and :

$$Y_{Eq} \simeq \frac{45\gamma_\psi}{4\pi^2} \eta_\psi \frac{x^2}{g_S} K_2(x), \quad (5.32)$$

where,  $\gamma_\psi = 2$  is the degeneracy factor,  $\eta_\psi = \exp(\mu_\psi/T) = 1$  (as  $\mu_\psi = 0$ ) is the factor which parametrizes the dependence of chemical potential on temperature,  $K_2(x)$  is the modified

Bessel function of order 2 and  $g_S$  is given as :

$$g_S = \sum_{i \in \text{bosons}} g_i \left( \frac{T_i}{T} \right)^3 + \frac{7}{8} \sum_{i \in \text{fermions}} g_i \left( \frac{T_i}{T} \right)^3. \quad (5.33)$$

We can appropriately choose the initial values and produce a graph for either the Freeze-Out or Freeze-in case. We can also plot the equilibrium distribution of dark matter to obtain a better idea of how the plots can look like.

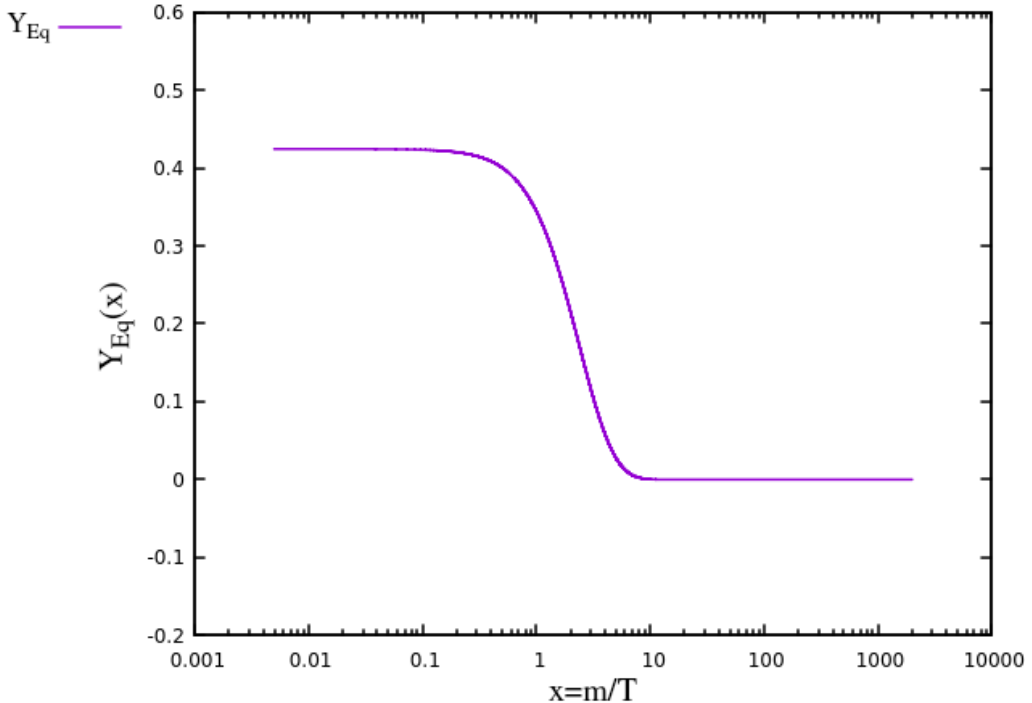


**Fig. 5.1:** Equilibrium distribution ( $Y_{eq}$ ) of Dark Matter obtained from plotting (5.32)

We observe that as  $x$  increases, that is  $T$  reduces as the Universe cools down due to expansion, the equilibrium density of dark matter goes down and ultimately becomes zero after a point. So, if dark matter is in equilibrium, its density falls to zero around  $x = 10$  value. For a dark matter of mass  $m = 100\text{GeV}$ , this corresponds to a temperature of  $T = 10\text{GeV}$ .

### 5.2.1 Freeze-Out Scenario

To obtain the solution for the Freeze-in case, we need to solve the equation (5.31) numerically and plot the results obtained. Before that, we need to establish the constants and initial conditions.

Setting the constants :

$$m_{Pl} = 1.221 \times 10^9 \text{GeV},$$

$$g_* = g_S = 10.75,$$

$$C_1 = \sqrt{\frac{8\pi^2}{45} g_*(x) m_{Pl}} = 1.671 \times 10^{20},$$

$$C_2 = \frac{45\gamma_\psi}{4\pi^2} \eta_\psi \frac{x^2}{g_S} = 0.021356,$$

$$m_\psi = 100 \text{GeV},$$

$$x_{\text{initial}} = 0.005 \implies T_{\text{initial}} = 2 \times 10^4 \text{GeV},$$

$$Y_{\text{initial}} = Y_{\text{Eq}}(x_{\text{initial}}).$$

We then use the RK4 method to numerically solve the differential equation for different values of  $\langle \sigma v \rangle$  to obtain the plot of  $\ln \left[ \frac{Y(x)}{Y(x=0)} \right]$  vs  $x = \frac{m}{T}$ .

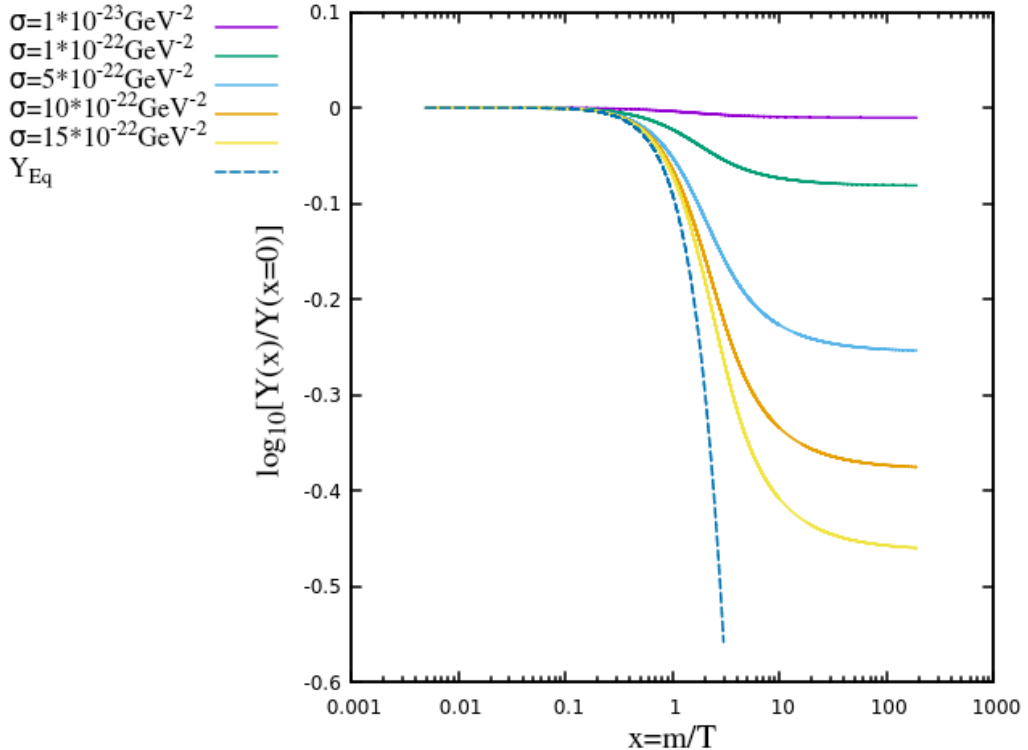


**Fig. 5.2:** Solution for dark matter yield, normalised to equilibrium yield, for  $m_\psi = 100 \text{GeV}$  by the freeze-out mechanism for different values of scattering cross section. The equilibrium yield plot is also shown for comparison.

Comparing the freeze-out of dark matter with its equilibrium distribution, we can see that the dark matter density branches out from the equilibrium density as the Universe expands and freezes out. We also observe that the yield remains equal to the equilibrium yield till some value of  $x$  (consequently till some temperature  $T$ ). As the Universe expands and cools down, the dark matter particles fall out of equilibrium. The sharpness of that fall and the final dark matter yield depends on how large the value of scattering cross section is. For very high scattering, that is stronger interactions, the remaining dark matter relic is much smaller when compared to weakly interacting dark matter with small scattering cross-sections.

### 5.2.2 Freeze-In Scenario

Here, we consider an alternate scenario in which the relic density of dark matter does not start with the equilibrium distribution. Instead the initial dark matter density is negligible, almost close to zero. Dark matter is formed due to collision of Standard Model particles and slowly increases in density. As time progresses, the dark matter density tries to obtain equilibrium distribution, while competing with the expansion of the Universe. Once the expansion rate dominates over the interaction length, the dark matter density freezes in with whatever density it could reach upto that point.

To solve for this case, we have to choose an initial value of yield ( $Y_{initial}$ ) such that it is almost close to zero but also supports the computational RK4 code.

We choose values  $Y_{initial} = 0.001$  and  $Y_{initial} = 10^{-5}$  and kept the rest of the constants same as before. It is a purely computational choice to ensure the smooth running of the RK4 code to solve the required differential equation. Both choices resulted in identical results, thus we choose to plot the results starting with lower yield value for more accuracy.

For comparison, I have also plotted the solution for equilibrium value of yield. Our results show that the yield tries to obtain equilibrium value as the Universe cools down.

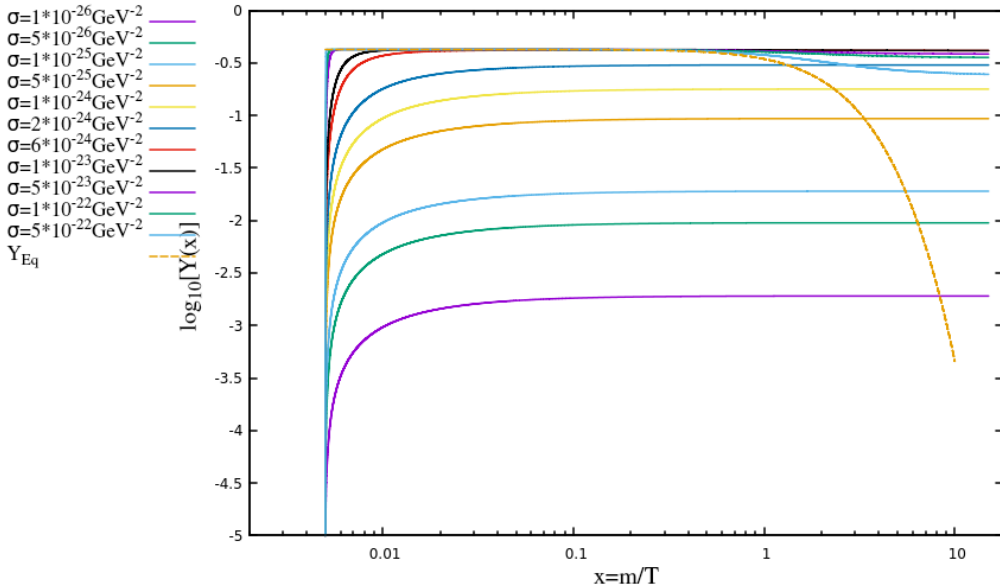


**Fig. 5.3:** Solution for yield for dark matter of  $m_\psi = 100\text{GeV}$  by the freeze-in mechanism for different values of scattering.

We see the trends of dark matter yield vary significantly between the two cases of freeze-in mechanism and freeze-out mechanism of dark matter formation. In the freeze-in case, we started with the assumption that the abundance before freeze-in is close to zero. We observe that as the value of  $x$  goes up, that is value of temperature goes down, the relic yield increases. For lower values of scattering cross section, the dark matter particle never comes into thermal equilibrium and the yield gets constant over time as the Universe expands. As

the mass is held constant, lower scattering cross section implies weakly interacting dark matter and vice versa. So, for stronger couplings, the relic yield formed also increases, until it reaches a strong enough coupling to enter into thermal equilibrium. Once it enters thermal equilibrium, eventually it decouples from the background and the yield gets constant like in the freeze-out case.

## 5.3 Axion Production in the Early Universe

The “Irreducible Axion Background” by Langhoff et al[16] works with an irreducible axion background in the Universe produced by the freeze-in mechanism, and they put constraints on axion-like particles in the mass range of 100eV-100MeV.

### 5.3.1 Solving the Boltzmann equation with relevant scattering processes

We consider an early Universe with reheating temperature as  $T_{RH} = 5\text{MeV}$ . This reheat temperature is defined as the temperature of the Universe when it enters the last phase of its radiation domination[16]. The interactions written in the Lagrangian (2.6) [16] can describe the process correctly till  $T_{RH} = 100\text{MeV}$ . After this temperature, additional degrees of freedom arise and the Lagrangian no longer remains an accurate picture. Within the allowed temperature range, we can production of axions in the Early Universe by primarily four main processes[16].

- I.) Photon Conversion :  $e^\pm \gamma \longrightarrow e^\pm a$
- II.) Electron-Positron Annihilation :  $e^- e^+ \longrightarrow \gamma a$
- III.) Photon Inverse Decay :  $\gamma \gamma \longrightarrow a$
- IV.) Electron-Positron Inverse Decay :  $e^- e^+ \longrightarrow a$

We now need to solve the Boltzmann equation discussed previously to get the accurate yield, as an effective fraction of dark matter, denoted by  $\mathcal{F}_a$ .

The Boltzmann equation derived (5.20) can be rewritten as[16] :

$$\frac{dY_a}{dx} = \frac{\tilde{g}(x)}{xH(x)s(x)} R(x) \quad (5.34)$$

where  $R(x)$  is the term encoding the scattering information and  $\tilde{g}(x) = 1 - \frac{1}{3} \frac{d \ln g_*}{d \ln x}$  [16]. We ignore all processes which can lead to depletion of axions, and we obtain the yield of axions given as [16]:

$$\mathcal{F}_a \simeq \frac{m_a s_0}{\rho_{DM}^0} Y_a(\infty) = \frac{m_a s_0}{\rho_{DM}^0} \int_{x_{RH}}^{\infty} dx \frac{\tilde{g}(x)}{xH(x)s(x)} R(x) \quad (5.35)$$

The contribution from all relevant processes can be directly added up as  $\mathcal{F}_a$  is linear in  $R(x)$ .

$R(x)$  for inverse decays ( $1 + 2 \rightarrow a$ ) can be written as [16] :

$$R_{1D}(T) = |\mathcal{M}_{1+2 \rightarrow a}|^2 \int d\Pi_1 d\Pi_2 d\Pi_a (2\pi)^4 \delta^4(p_1 + p_2 - p_a) \times f_a^{eq} [1 \pm (f_1^{eq} + f_2^{eq})] \quad (5.36)$$

with scattering amplitudes  $|\mathcal{M}_{1+2 \rightarrow a}|^2$  calculated in the previous chapter (2.16,2.21).

Similarly for the two-to-two scattering, we can estimate the scattering amplitudes and solve  $R(x)$  numerically [16]:

$$R_{2 \rightarrow 2}(T) = |\mathcal{M}_{1+2 \rightarrow 3+a}|^2 \int d\Pi_1 d\Pi_2 d\Pi_3 d\Pi_a (2\pi)^4 \delta^4(p_1 + p_2 - p_3 - p_a) \times e^{-(E_1 + E_2)/T} \quad (5.37)$$

The equations need to solved for different values of  $g_{a\gamma\gamma}$  (photophilic axions) or  $g_{aee}$  (photophobic axions) and mass of the axion  $m_a$ . For each set of value we would have a solution for  $\mathcal{F}_a$ . The results can then be combined to form a contour graph[16] of axion yield as a function of mass of axion and interaction strength of axion with photon or electron.

Photophilic axions are the class or model of axions which couple to photons but have no coupling to electrons or positrons, i.e.,  $g_{aee} = 0$  and  $g_{a\gamma\gamma} \neq 0$ . Photophobic axions is the class or model of axions with no coupling to photons but coupling to other Standard Model particles, which are electrons and positrons here, i.e.,  $g_{aee} \neq 0$  and  $g_{a\gamma\gamma} = 0$ .

The density of axions produced by the freeze-in process here is considered to be the irreducible axion background since it is assumed that at the instance of reheating, the axion density was zero ( $\rho_a = 0$ ) and abundance is accumulated after reheating. Any further assumption about the state of the Universe before reheating can only result in an increase in the density of axions. Thus, the density obtained by these assumptions gives us the irreducible axion density.

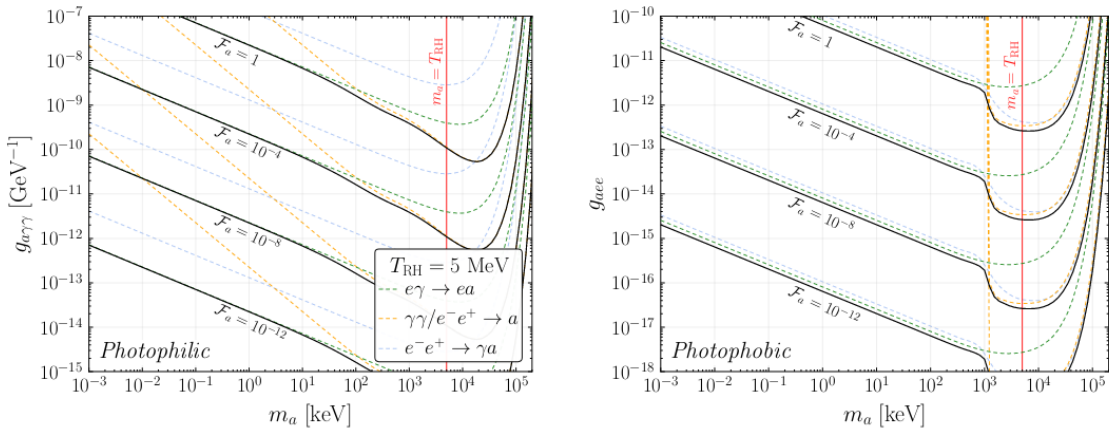


**Fig. 5.4:** Contours of constant effective dark matter fraction  $\mathcal{F}_a$  for photophilic (left) and photophobic (right) axions for reheat temperature of  $T_{RH} = 5\text{ MeV}$ . The black line shows contours of  $\mathcal{F}_a$  which are the sum of all relevant processes considered. The dashed green line shows contribution from photon conversion, the dashed orange line shows contribution from inverse decays and the dashed blue lines show contribution from annihilations.[16]

The equations (5.35) with (5.36) and (5.37) have been solved and plotted into a contour graph by Langhoff et al, which I have attached above [16] in Fig(5.4).

We can infer from the above plot that in the case of  $m_a \ll T_{RH}$ , the photon conversion process dominates the produced yield of axions while for  $m_a \geq T_{RH}$  the process of inverse decays starts dominating the production. The fermion annihilation process is always subdominant. The sharp kink in the graph for photophobic axions mark the scale at which mass of the axion becomes approximately equal to 1MeV (mass of two electrons, or electron positron pair). At that point the inverse decay of electron and positron is turned on and then starts becoming the dominant mode as we move towards higher mass of axion  $m_a$ . The electron-positron inverse decay contributes to the production of axions only for mass of axions larger than 1MeV[16].

**Conclusion :** Axions as possible dark matter candidates can be produced in the early Universe by the freeze-in mechanism. At different mass ranges different conversions or reactions control the production of axions. The relic density of axions obtained here at reheat temperature of  $T_{RH} = 5\text{MeV}$  are now used in the next chapter to obtain constraints on axion-photon and axion-electron couplings.

# Chapter 6

## Constraints on Axion-Like Particles

In this chapter, I will attempt to summarise the arguments put forward by Langhoff et al[16] to obtain stronger constraints on axion-like particles.

### 6.1 The Irreducible Axion Background

The paper focuses on the scenario where axions are produced without reaching thermal equilibrium. This will form a relic contribution to density of dark matter  $\rho_{DM}$ . To ensure that the abundance obtained is as small as possible, the lowest possible value of reheating temperature is taken and at the time of reheating, the density of axions is taken to be 0, i.e.,  $\rho_a(T = T_{RH}) = 0$ . Using these assumptions, the axion density obtained becomes an irreducible density as any change in these assumptions will lead to only increase of the density. The minimal reheating temperature is chosen to be 5MeV.[16]

When the reheating temperature of the Universe is around 5MeV, then at that epoch the Standard Model plasma contained electrons, positrons, photons and neutrinos. Freeze-in is considered to be the relevant mode of axion production. Then, the axion density can be written as :

$$\rho_a = \exp\left(-\frac{t}{\tau}\right) \mathcal{F}_a \rho_{DM}. \quad (6.1)$$

The exponential term accounts for the decays of axions which leads to depletion of the density. Using the definition of  $\rho_a$ , we can define  $\mathcal{F}_a$ , the effective dark matter fraction as :

$$\mathcal{F}_a = \exp\left(\frac{t_U}{\tau_a}\right) \frac{\rho_{a,0}}{\rho_{DM,0}}, \quad (6.2)$$

where,  $t_U$  is the lifetime of the Universe and it shows up because the dark matter has a lifetime more than or comparable to the lifetime of the Universe. In the previous chapter, I discussed the process of obtaining  $\mathcal{F}_a$  and showed the resulting contours in Fig(5.4).

Even though we have the full solutions for  $\mathcal{F}_a$ , we can make some limiting approximations to

better understand the results. Assuming  $m \leq T_{RH}$ ,  $m_a < 2m_e$  and setting  $g_* = 10.75$ , we obtain expressions for  $\mathcal{F}_a$  for the photophobic and photophilic case as[16] :

$$\mathcal{F}_{a\gamma} \simeq 0.20 \left( \frac{m_a}{\text{keV}} \right) \left( \frac{g_{a\gamma\gamma}}{10^{-8}\text{GeV}^{-1}} \right)^2 \left( \frac{T_{RH}}{5\text{MeV}} \right), \quad (6.3)$$

$$\mathcal{F}_{ae} \simeq 2.4 \left( \frac{m_a}{\text{keV}} \right) \left( \frac{g_{aee}}{10^{-10}\text{GeV}^{-1}} \right)^2. \quad (6.4)$$

In this scenario, the decay rates are given as :

$$\tau_{a\gamma\gamma}^{(\gamma)} \simeq 3.0 \times 10^6 t_U \left( \frac{m_a}{\text{keV}} \right)^{-3} \left( \frac{g_{a\gamma\gamma}}{10^{-8}\text{GeV}^{-1}} \right)^{-2}, \quad (6.5)$$

$$\tau_{a\gamma\gamma}^{(e)} \simeq 1.4 \times 10^{10} t_U \left( \frac{m_a}{\text{keV}} \right)^{-7} \left( \frac{g_{aee}}{10^{-8}\text{GeV}^{-1}} \right)^{-2}. \quad (6.6)$$

## 6.2 Constraints from Axion Decays

The couplings of axions to photons and electrons which lead to the production of their relic density also mediate their decays at a later time in the Universe. We can specifically consider the case of  $m_a \ll m_e$ , in which scenario axion only decays to photons, via a triangle diagram mediated by electrons. As shown in chapter 2, the decay rate in this scenario can be written as (2.27)[16]:

$$\Gamma_{a \rightarrow \gamma\gamma} = \frac{m_a^3}{64\pi} \left[ g_{a\gamma\gamma} + \frac{\alpha g_{aee} m_a^2}{12m_e^3 \pi} \right]. \quad (6.7)$$

We next make the assumption that axions behave exactly like cold DM. Then, we take into consideration the constraints existing on dark matter from currently known experiments.

Let us look at the constraints on dark matter decaying to two photons locally, say in the Milky Way. The differential photon flux from such dark matter decays can be written as [16]:

$$\frac{d\Phi}{dE} = \frac{D}{2\pi m_{DM} \tau_{DM}} \delta \left( E - \frac{m_{DM}}{2} \right). \quad (6.8)$$

Here,  $m_{DM}$  is the mass of the dark matter,  $\tau_{DM}$  is the inverse decay rate of dark matter going to two photons. The D-factor is obtained by integrating the dark matter mass column density over the line of sight.

$$D = \int dz d\Omega \rho_{DM}(z, \Omega), \quad (6.9)$$

where,  $z$  is the distance along the line of sight and  $\Omega$  is the solid angle. If an instrument does not make any observations, then we can interpret that result as a constraint on the minimal allowed lifetime at that particular mass value. We denote this constraint value as  $\tau_{DM}^{\min}$ .

We can now focus on axionic relic density as dark matter. The irreducible axion density can also produce photon flux in the Universe which we may observe. We can calculate this flux of

## 6.2. CONSTRAINTS FROM AXION DECAYS

---

photons by making the following replacements in (6.6)[16] :

$$m_{DM} \longrightarrow m_a \quad ; \quad \tau_{DM} \longrightarrow \tau_{a \rightarrow \gamma\gamma} \quad ; \quad D \longrightarrow \mathcal{F}_a e^{(-t_U/\tau_a)} D. \quad (6.10)$$

We can then recast the constraints on dark matter coupling to give us constraints on the inverse decay rate of axions, which in turn give us constraints on axion coupling strength to electrons and photons via (6.5) and (6.6). We can write these constraints as [16] :

$$\mathcal{F}_a \leq \mathcal{F}_{\text{local}}^{\max} \equiv \frac{\tau_{a\gamma\gamma}}{\tau_{DM}^{\min}} \exp\left(\frac{t_U}{\tau_a}\right). \quad (6.11)$$

The lower limit on the constraints are given by the condition [16] :

$$\frac{\tau_{a\gamma\gamma}}{\mathcal{F}_a} \sim \tau_{DM}^{\min}. \quad (6.12)$$

The upper boundary is realised when  $\tau_a \ll t_U$ , as in this case, from the definition of  $\mathcal{F}_a$  in (6.2), it becomes exponentially large. Thus, the local dark matter density gets exponentially suppressed below  $\mathcal{F}_a$ .

Observations of CMB anisotropies also allows us to probe decays at earlier times and put constraints on the parameter space[16].

$$\mathcal{F}_a \leq \mathcal{F}_{CMB}^{\max} \equiv \frac{\tau_a}{\tau_{CMB}^{\min}} \exp\left(\frac{t_{CMB}}{\tau_a}\right)^{2/3}. \quad (6.13)$$

The constraints on  $\tau_{DM}^{\min}$ , which in turn give constraints on  $\tau_a$  are obtained from experiments like XMM-Newton [27, 28, 29], NuSTAR[30, 31, 32] and INTEGRAL[33]. These bounds are valid in the mass range of 100eV to 100MeV.

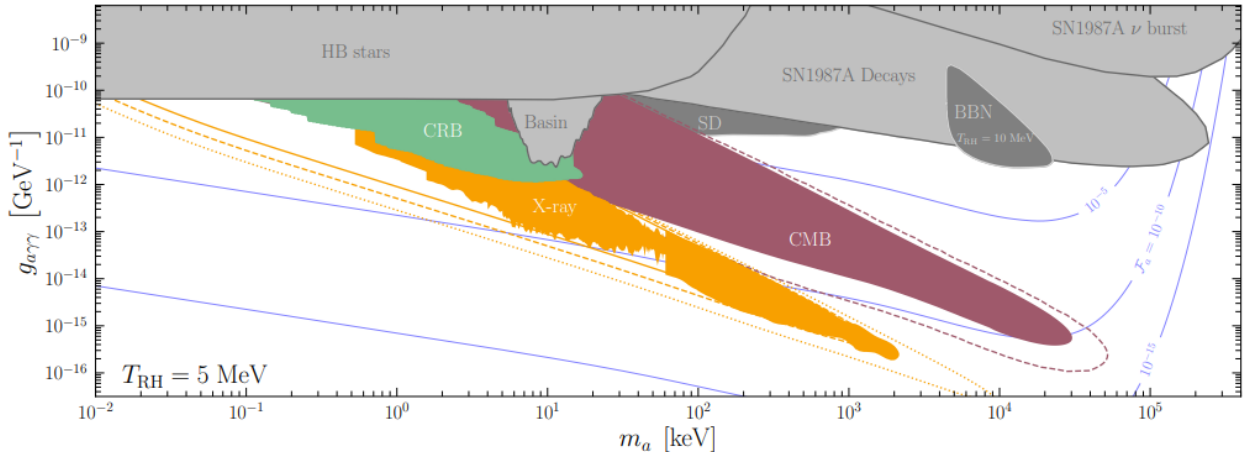


**Fig. 6.1:** Constraints on Photophilic axion's mass and coupling for irreducible case of  $T_{RH} = 5$  MeV. Plot taken from Langhoff et al [16]

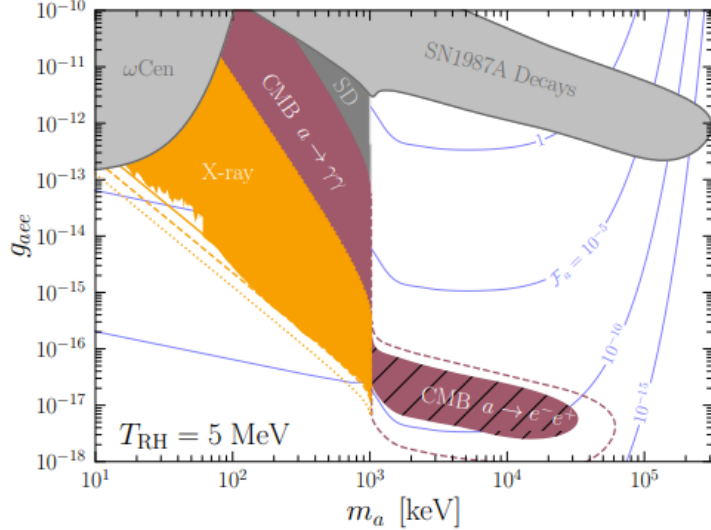


**Fig. 6.2:** Constraints on Photophobic axion's mass and coupling for irreducible case of  $T_{RH} = 5\text{ MeV}$ . Plot taken from Langhoff et al [16]

At around 10keV, the bounds obtained from this work become three orders of magnitude stronger than the existing bound on axion-photon coupling which has been established using data from horizontal branch stars. This allows us to write[16] :

$$g_{a\gamma\gamma} \leq 8.1 \times 10^{-14}\text{GeV}^{-1}. \quad (6.14)$$

While the results have been presented for a fixed value of reheating temperature, the paper also provides a discussion on effect of reheating temperature on the results. If the mass is fixed, with  $m_a \ll T_{RH}$ , then increasing  $T_{RH}$  only changes the results by a small amount.  $g_{a\gamma\gamma}$  gets affected as inverse one fourth of the reheating temperature, i.e.,  $g_{a\gamma\gamma} \propto T_{RH}^{-1/4}$ .

For the case of photophobic axions, a bound almost four orders of magnitude stronger than earlier known results is obtained in [16] for axion-like particle of mass 100keV. This allows us to write :

$$g_{aee} \leq 8.0 \times 10^{-15}\text{GeV}^{-1}. \quad (6.15)$$

Thus, axions or axion-like particles in the mass range of 100eV to 100MeV can be produced sufficiently, and can also form a fraction of dark matter which is detectable.

**Conclusion :** Considering the irreducible density of axions to be produced by the freeze-in mechanism, there are two main conclusions that we arrive at. First, axions produced by this mechanism constitute only a very small fraction of the total dark matter density. Secondly, using the existing constraints on dark matter, we can put constraints on interactions of axions to photons and electrons. These new constraints are many orders of magnitude stronger than the previous constraints obtained previously by studying horizontal branch stars, the CMB and so on.

# Chapter 7

## Conclusion

The Strong CP problem is one of the prominent problems of particle physics which deals with the non-violation of CP symmetry in Quantum Chromodynamics. The problem can be solved dynamically by promoting the CP violating parameter to be a field instead of a constant number. This field has an  $U(1)_{PQ}$  symmetry associated with them. When this  $U(1)_{PQ}$  symmetry gets broken, the field obtains some minimum value, which removes the CP violating term from the Lagrangian, thereby solving the Strong CP problem. Such fields are known as axion fields.

There can be different types of axion models which can be characterised by their symmetry breaking scales amongst other things. Axion models with symmetry breaking scales at around the electroweak symmetry breaking scale of around 250GeV are known as the Peccei-Quinn-Weinberg-Wilczek (PQWW) axion models. In these models, an extra Higgs field is added to the QCD Lagrangian, making a total of two Higgs field in the model. The PQWW axions would have mass in the order of 100keV and coupling such that it would be large enough to be detected by collider experiments. But these PQWW axion models have been experimentally ruled out by beam-dump experiments and recent collider experiments.

Another class of axion models is known as “invisible” axion models which have a symmetry breaking scale much larger than the electroweak symmetry breaking scale of 250GeV. Due to this, the axion has considerably decreased mass and coupling. These “invisible” axions have very weak interactions with the other Standard Model particles. As a result of this, these “invisible” axion models can be possible dark matter candidates.

Dark matter is a hypothetical form of matter which constitutes 85% of the matter of the Universe. It has no interaction with the electromagnetic field, hence it is known as “dark” matter. It only interacts with other matter via the gravitational field. Several observational evidences, like galaxy rotation curves and the bullet cluster to support the existence of dark matter. From observations and theories, we know that dark matter has to be “cold”, i.e., they need to have non-relativistic populations along with extremely weak interactions to Standard Model particles. The “invisible” axions can be produced in the Universe by the misalignment

---

mechanism. The axion population thus produced is non-relativistic, and is non-zero at present time. Since these axion models have very low interactions, the population produced does not decay away completely and thus axions could be viable dark matter candidates.

Dark matter can be produced in the Universe by either the Freeze-out mechanism or the Freeze-in mechanism. The yield of dark matter produced can be obtained by solving the general Boltzmann equation for the freeze-out and the freeze-in case. The discussion can also be specialised to axion-like particles (ALPs) and their yield can be obtained if we know the scattering amplitude of axions with Standard Model particles. For the thesis, I have focussed on interaction of axions only with photons and electrons. Considering all the possible scattering channels, we come to the conclusion that at different mass ranges, different conversion processes control axion production. For mass of the axion lesser than the reheat temperature of the Universe, the process of photon conversion dominates the yield, while for mass greater than the reheat temperature inverse decay processes stars dominating the yield of axions. The results discussed are for reheat temperature  $T_{RH} = 5\text{MeV}$ .

Considering the yield of axion produced to be a part of dark matter, we first observe that axions form a very small fraction of dark matter. Then, using the existing constraints on dark matter, we can put constraints on the interaction strength of axions to photons and electrons. These constraints are three to four orders of magnitude stronger than the ones previously known from studies of horizontal branch stars, CMB, SN1987A decays and so on.

# Bibliography

- [1] R. D. Peccei, “The strong CP problem and axions,” in *Lecture Notes in Physics*, pp. 3–17, Springer Berlin Heidelberg, 2008.
- [2] M. E. Peskin and D. V. Schroeder, *An Introduction to quantum field theory*. Reading, USA: Addison-Wesley, 1995.
- [3] R. D. Peccei and H. R. Quinn, “CP conservation in the presence of pseudoparticles,” *Phys. Rev. Lett.*, vol. 38, pp. 1440–1443, Jun 1977.
- [4] F. Wilczek, “Problem of Strong  $P$  and  $T$  Invariance in the Presence of Instantons,” *Phys. Rev. Lett.*, vol. 40, pp. 279–282, 1978.
- [5] S. Weinberg, “A new light boson?,” *Phys. Rev. Lett.*, vol. 40, pp. 223–226, Jan 1978.
- [6] D. J. Marsh, “Axion cosmology,” *Physics Reports*, vol. 643, pp. 1–79, jul 2016.
- [7] J. E. Kim, “Light pseudoscalars, particle physics and cosmology,” *Physics Reports*, vol. 150, no. 1, pp. 1–177, 1987.
- [8] K. Mimasu and V. Sanz, “Alps at colliders,” 2014.
- [9] J. E. Kim, “Weak Interaction Singlet and Strong CP Invariance,” *Phys. Rev. Lett.*, vol. 43, p. 103, 1979.
- [10] M. A. Shifman, A. I. Vainshtein, and V. I. Zakharov, “Can Confinement Ensure Natural CP Invariance of Strong Interactions?,” *Nucl. Phys. B*, vol. 166, pp. 493–506, 1980.
- [11] M. Dine, W. Fischler, and M. Srednicki, “A Simple Solution to the Strong CP Problem with a Harmless Axion,” *Phys. Lett. B*, vol. 104, pp. 199–202, 1981.
- [12] A. R. Zhitnitsky, “On Possible Suppression of the Axion Hadron Interactions. (In Russian),” *Sov. J. Nucl. Phys.*, vol. 31, p. 260, 1980.
- [13] H. Primakoff, “Photo-production of neutral mesons in nuclear electric fields and the mean life of the neutral meson,” *Phys. Rev.*, vol. 81, pp. 899–899, Mar 1951.
- [14] G. G. Raffelt, “Plasmon decay into low-mass bosons in stars,” *Phys. Rev. D*, vol. 37, pp. 1356–1359, Mar 1988.

- [15] S. Andriamonje, S. Aune, D. Autiero, K. Barth, A. Belov, B. Beltrá n, H. Bräuninger, J. M. Carmona, S. Cebrián, J. I. Collar, T. Dafni, M. Davenport, L. D. Lella, C. Eleftheriadis, J. Englhauser, G. Fanourakis, E. F. Ribas, H. Fischer, J. Franz, P. Friedrich, T. Geralis, I. Giomataris, S. Gninenko, H. Gómez, M. Hasinoff, F. H. Heinsius, D. H. H. Hoffmann, I. G. Irastorza, J. Jacoby, K. Jakovčić, D. Kang, K. Königsmann, R. Kotthaus, M. Krčmar, K. Kousouris, M. Kuster, B. Lakić, C. Lasseur, A. Liolios, A. Ljubičić, G. Lutz, G. Luzón, D. Miller, A. Morales, J. Morales, A. Ortiz, T. Papaevangelou, A. Placci, G. Raffelt, H. Riege, A. Rodríguez, J. Ruz, I. Savvidis, Y. Semertzidis, P. Serpico, L. Stewart, J. Vieira, J. Villar, J. Vogel, L. Walckiers, K. Zioutas, and C. Collaboration, “An improved limit on the axion–photon coupling from the CAST experiment,” *Journal of Cosmology and Astroparticle Physics*, vol. 2007, pp. 010–010, apr 2007.
- [16] K. Langhoff, N. J. Outmezguine, and N. L. Rodd, “The irreducible axion background,” 2022.
- [17] A. Hook, “Tasi lectures on the strong cp problem and axions,” 2018.
- [18] L. D. Duffy and K. van Bibber, “Axions as dark matter particles,” *New Journal of Physics*, vol. 11, p. 105008, oct 2009.
- [19] G. G. Raffelt, *Stars as laboratories for fundamental physics: The astrophysics of neutrinos, axions, and other weakly interacting particles*. 5 1996.
- [20] S. Profumo, L. Giani, and O. F. Piattella, “An introduction to particle dark matter,” 2019.
- [21] E. Corbelli and P. Salucci, “The extended rotation curve and the dark matter halo of m33,” *Monthly Notices of the Royal Astronomical Society*, vol. 311, pp. 441–447, jan 2000.
- [22] M. Markevitch, A. H. Gonzalez, D. Clowe, A. Vikhlinin, L. David, W. Forman, C. Jones, S. Murray, and W. Tucker, “Direct constraints on the dark matter self-interaction cross-section from the merging galaxy cluster 1E0657-56,” *Astrophys. J.*, vol. 606, pp. 819–824, 2004.
- [23] W. Tucker, P. Blanco, S. Rappoport, L. David, D. Fabricant, E. E. Falco, W. Forman, A. Dressler, and M. Ramella, “1e 0657-56: A contender for the hottest known cluster of galaxies,” *The Astrophysical Journal*, vol. 496, pp. L5–L8, mar 1998.
- [24] P. Sikivie, “Axion cosmology,” in *Lecture Notes in Physics*, pp. 19–50, Springer Berlin Heidelberg, 2008.
- [25] S. Chang, C. Hagmann, and P. Sikivie, “Studies of the motion and decay of axion walls bounded by strings,” *Physical Review D*, vol. 59, dec 1998.
- [26] E. W. Kolb and M. S. Turner, *The Early Universe*, vol. 69. 1990.

- [27] J. W. Foster, M. Kongsore, C. Dessert, Y. Park, N. L. Rodd, K. Cranmer, and B. R. Safdi, “Deep Search for Decaying Dark Matter with XMM-Newton Blank-Sky Observations,” *Phys. Rev. Lett.*, vol. 127, no. 5, p. 051101, 2021.
- [28] A. Boyarsky, A. Neronov, O. Ruchayskiy, M. Shaposhnikov, and I. Tkachev, “Where to find a dark matter sterile neutrino?,” *Phys. Rev. Lett.*, vol. 97, p. 261302, 2006.
- [29] A. Boyarsky, J. Nevalainen, and O. Ruchayskiy, “Constraints on the parameters of radiatively decaying dark matter from the dark matter halo of the Milky Way and Ursa Minor,” *Astron. Astrophys.*, vol. 471, pp. 51–57, 2007.
- [30] K. C. Y. Ng, B. M. Roach, K. Perez, J. F. Beacom, S. Horiuchi, R. Krivonos, and D. R. Wik, “New Constraints on Sterile Neutrino Dark Matter from *NuSTAR* M31 Observations,” *Phys. Rev. D*, vol. 99, p. 083005, 2019.
- [31] B. M. Roach, K. C. Y. Ng, K. Perez, J. F. Beacom, S. Horiuchi, R. Krivonos, and D. R. Wik, “Nustar tests of sterile-neutrino dark matter: New galactic bulge observations and combined impact,” *Phys. Rev. D*, vol. 101, p. 103011, May 2020.
- [32] B. M. Roach, S. Rossland, K. C. Y. Ng, K. Perez, J. F. Beacom, B. W. Grefenstette, S. Horiuchi, R. Krivonos, and D. R. Wik, “Long-exposure NuSTAR constraints on decaying dark matter in the Galactic halo,” *Phys. Rev. D*, vol. 107, no. 2, p. 023009, 2023.
- [33] F. Calore, A. Dekker, P. D. Serpico, and T. Siegert, “Constraints on light decaying dark matter candidates from 16 yr of INTEGRAL/SPI observations,” *Mon. Not. Roy. Astron. Soc.*, vol. 520, no. 3, pp. 4167–4172, 2023.
- [34] E. Corbelli and P. Salucci, “The extended rotation curve and the dark matter halo of M33,” *Monthly Notices of the Royal Astronomical Society*, vol. 311, pp. 441–447, 01 2000.
- [35] K. van Bibber, P. M. McIntyre, D. E. Morris, and G. G. Raffelt, “Design for a practical laboratory detector for solar axions,” *Phys. Rev. D*, vol. 39, pp. 2089–2099, Apr 1989.
- [36] P. Sikivie, “Experimental tests of the ”invisible” axion,” *Phys. Rev. Lett.*, vol. 51, pp. 1415–1417, Oct 1983.
- [37] M. Dutra, *Origins for dark matter particles : from the ”WIMP miracle” to the ”FIMP wonder”*. PhD thesis, Orsay, LPT, 2019.